Measuring Land Subsidence with PS-InSAR in Bangkok using Sentinel-1 Time-Series Techniques

SAWITREE LUACHAPICHATIKUL

A THESIS SUBMITTED IN PARTIAL FULFILLMENT OF
THE REQUIREMENTS FOR MASTER OF SCIENCE
IN GEOINFORMATICS
FACULTY OF GEOINFORMATICS
BURAPHA UNIVERSITY
2020

การวัดอัตราการทรุดตัวของแผ่นดินด้วย PS-InSAR บริเวณกรุงเทพมหานคร โดยใช้ดาวเทียมเรดาร์ Sentinel-1 Time-series Techniques

สาวิตรี ลือชาอภิชาติกุล

วิทยานิพนธ์นี้เป็นส่วนหนึ่งของการศึกษาตามหลักสูตรวิทยาศาสตรมหาบัณฑิต
สาขาวิชาภูมิสารสนเทศศาสตร์
คณะภูมิสารสนเทศศาสตร์ มหาวิทยาลัยบูรพา
2563

Measuring Land Subsidence with PS-InSAR in Bangkok using Sentinel-1 Time-Series Techniques

SAWITREE LUACHAPICHATIKUL

A THESIS SUBMITTED IN PARTIAL FULFILLMENT OF
THE REQUIREMENTS FOR MASTER OF SCIENCE
IN GEOINFORMATICS
FACULTY OF GEOINFORMATICS
BURAPHA UNIVERSITY
2020

The thesis of Sawitree Luachapichatikul has been approved by the examining committee to be partial fulfillment of the requirements for the Master of Science in Geoinformatics of Burapha University

Advisory Committee

Principal Advisor

(Professor Timo Balz)

Examining Committee

(Professor Shi Lei) Principal examiner

Member
(Professor Shao Zhenfeng)

External member
(Associate Professor Jianzhong Lu)

External member
(Dr. Tanita Suepa)

(Lecturer Dr. Kitsanai Charoenjit)
Dean of the Faculty of Geoinformatics
14 May 2021

This thesis has been approved by Graduated School Burapha University to be partial fulfillment of the requirements for the Master of Science in Geoinformatics of Burapha University

(Associate Professor Dr. Nujjaree Chaimongkol)
Dean of Graduated School
8 June 2021

61910094: MAJOR: GEOINFORMATICS; M.Sc. (GEOINFORMATICS)

KEYWORDS: Bangkok, Land subsidence, PS-InSAR, Sentinel-1, SARPROZ, Geological subsidence

SAWITREE LUACHAPICHATIKUL :

MEASURING LAND SUBSIDENCE WITH PS-INSAR IN BANGKOK USING SENTINEL-1 TIME-SERIES TECHNIQUES. ADVISORY COMMITTEE: TIMO BALZ, , PATTAMA PHODEE SUKONMETH JITMAHANTAKUL 2020.

Bangkok, the capital city of Thailand, has been affected by land subsidence since early 1970. Subsidence related factors are analyzed, including groundwater over-exploitation, aquifer structure, crustal deformation, urban construction, land use types, and clay thickness. These different factors have effects on the urban area and can lead to hazardous consequences. Nowadays, the space-borne Synthetic Aperture Radar (SAR) can detect structural deformation due to several phenomena of the Earth's surface. SAR images offer high resolution, high observation density, high accuracy, resource-saving and are cost-effective for subsidence estimation. The Sentinel-1 radar satellite open data acquires data systematically and frequently over the Earth.

The questions analyzed in this study are: what PS-InSAR techniques measure and how can the land subsidence rate (mm/year) in Bangkok be derived from Sentinel-1 satellite image? What are the main factors of subsidence that influence/induce on Bangkok subsidence? Therefore, this study aims to apply the PS-InSAR time-series technique to measure the relative velocity (mm/year) and vertical movement (mm/year) of land subsidence in Bangkok and its surrounding area during 2016 until 2019. The study area consists of 3,450 sq.km in 80 ascending images and 3,450 sq.km in 93 descending images, and both areas include Bangkok city. The total study area covers Bangkok and also some part of Pathum Thani, Nonthaburi, Samut Sakhon, Samut Prakan, Nakhon Nayok, Chachoengsao, Ratchaburi, as well as Nakhon Pathom provinces in Thailand.

The land subsidence was measured by using PS-InSAR time-series techniques. Furthermore, it compares the subsidence from the descending orbit in the

Western Greater Bangkok and validates the relative movement between descending PS-InSAR results and the leveling survey technique in the study area. Lastly, the objective is to evaluate the performance of Sentinel-1 PS-InSAR time-series techniques from the intersection area of ascending and descending orbit, whereby the vertical velocity is decomposed from deformation along with the line-of-sight directions. The vertical velocity can correlate analysis of the geological subsidence with a spatial pattern of the PS-InSAR time-series techniques in Bangkok city.

The advantage of the PS-InSAR technique is suitable for detecting the point-like stable object and strong reflectors for estimating ground surface movement. So, the PS-InSAR time-series result was validated by using the depth of leveling benchmark that is more than or equals to 20 meters below the surface in ascending and descending orbits of research areas because the ground surface movement affects the construction in an urban area that is built of foundation engineering through the sedimentary bed in Quaternary basin.

The PS-InSAR Sentinel-1 time-series processing was administered in the SARPROZ software. The R-squared (RSQ) and standard deviation (σ) are used to validate the relative velocity between the PS-InSAR and leveling techniques. Additionally, the correlation pattern between subsidence and geology-geomorphology at the hexagonal area of interest of ascending orbit and descending orbit also relates to the vertical movement in this area.

The PS-InSAR result shows that the study area has been subsiding at the relative rate of 8-25 mm/year in the line-of-sight direction. 80 points/km^2 of 276,774 PS points, a stable point in the ascending area are detected. 232,814 PS points, with a density of 67 points/km^2 are detected as a stable point in the descending area. Nevertheless, limitation of PS subsidence point estimating can be related to the stable material, building, construction or less vegetation. The validate analysis between PS-InSAR and leveling benchmarks as a result of the analysis revealed four points benchmarks satisfyingly agree with the result from the PS-InSAR point. While the trendline of the BKK6062 benchmark point and PSI95832 PS-InSAR time-series point that both trendlines conform to the ninety-five-confidence interval, but the 95-confidence interval trendline is rather wide owing to the dispersion of leveling survey

points. It could be an error from leveling survey because it showed a low R-squared equal to 0.1, or phase unwrapping, microwave double-bounce, et cetera from PS-InSAR time-series technique.

The decomposed vertical velocity analysis revealed an area approximately 1700 sq.km within the interesting hexagonal area showing subsidence of averaging 8.93 mm/year and exceeding 20.01 mm/year in 2016-2019. Extreme subsidence occur at Khok Krabue, Bang Nam Chuet, and Phanthai Norasing in Mueang Samut Sakhon, Samut Sakhon province, as significant subsidence in red risk zone area. Because these areas are underlaid by soft Bangkok clay (Qa, Qc) and are accommodated by agriculture land use, aquaculture, industrial factories, and residential zone. Furthermore, it is for this reason that these areas have used groundwater overexploitation in substantial land subsidence. The groundwater level is a significant part of the factor for the observed subsidence, but the stratigraphic and the morphostructural setting in Bangkok's Quaternary basin is an important factor as well.

ACKNOWLEDGEMENTS

This thesis is a two-year result of the upskill and reskill in Master Dissertation of the Sirindhorn Center of Geo-Informatics (SCGI) Master's Program that is a collaboration amongst Wuhan University: China, Burapha University: Thailand, and GISTDA (under Ministry of Higher Education, Science, Research and Innovation: Thailand) to offer a Double Master Degree on Geo-Informatics and Space Technology. I also got government scholarships from the Ministry of Higher Education, Science, Research and Innovation, Thailand.

I have been accompanied and supported by many people. It is a pleasure that I now have the opportunity to express my gratitude to all of them. First, I would like to thank and appreciate my supervisor Prof.Dr.Ing- Timo Balz, co-advisor Dr. Pattama Phodee, and co-advisor Dr. Sukonmeth Jitmahantakul. I would also like to grateful the others members of my collage' s SCGI Master Program Student and the other members of my Master's, Ph.D. classmate and SAR team in Faculty of Geoinformatics, Burapha University and State Key Laboratory of Information Engineering in Surveying, Mapping and Remote Sensing, Wuhan University. The second special thanks go to Perssis SARPROZ software for the support software of land subsidence processing and the Royal Thai Survey Department for support data of subsidence measurement form leveling. I would like to personally thank to SARPROZ team who let me use their software and Col.Dr. Didsaphan Naksen for their kindly cooperation on the leveling survey data used in this thesis.

Finally, I am forever indebted to my mother, my brother, and my colleague, for their constant support, encouragement, and guidance.

Sawitree Luachapichatikul

TABLE OF CONTENTS

Page

LIST OF TABLES

Page

LIST OF FIGURES

Page

LIST OF SYMBOLS

ϕ	*Phase*
λ	*Wavelength*
θ	*Incidence Angle*
$\Delta\phi$	*Interferometric phase (or phase difference)*
ϕ_{def}	*Phase contribution related to ground deformation*
ϕ_{orbit}	*Orbit Error*
ϕ_{topo}	*Topographic Effect*
ϕ_{noise}	*Noise*
ϕ_{atm}	*Atmospheric Delay*
ϕ_1, ϕ_2	*The phase of each acquisition*
Δr	*The difference in range (LOS) between two SAR acquisitions*
d_{LOS}	*Deformation along line of sight (LOS)*
d_{Vert}	*Vertical motion*
d_{HALD}	*Horizontal in descending ALD*
$\Delta\alpha$	*Difference of the heading satellite between ascending and descending orbits*
σ	*Standard deviations*

LIST OF ACRONYMS AND ABBREVIATIONS

ALD Azimuth Look Direction

AOI Area of Interesting

APS Atmospheric phase screen

ASC Ascending orbit

ASI Agenzia Spaziale Italiana (Italian Space Agency)

BMA Bangkok Metropolitan Administration

CGPS Continuous Global Positioning System

CONAE Comisio ´n Nacional de Actividades Espaciales (Argentina - National Space Activities Commission)

CSA Canadian Space Agency

DCP Department of City Planning

DEM Digital Elevation Model

DES Descending orbit

DGR Department of Groundwater Resources

DInSAR Difference Interferometric Synthetic Aperture Radar

DLR Deutsches Zentrum fur Luft- und Raumfahrt (German Aerospace Centre)

DMR Department of Mineral Resources

ERS European remote sensing satellite

ESA European Space Agency

EW Extra-Wide swath

GCP Ground control point

GEO2TECDI-SONG Technologies for Thailand: Environment Change Direction and Investigation-Sea Offensive Next Generation

GIS Geographic Information Systems

GISTDA Geo-Informatics and Space Technology Development Agency

GMES Global Monitoring for Environment and Security

GNSS Global Navigation Satellite System

InSAR Interferometric Synthetic Aperture Radar

INTA Instituto Nacional de Te ´cnica Aeroespacial (Spain - National Institute of Aerospace Technology)

IW Interferometric Wide Swath

JAXA Japan Aerospace Exploration Agency

JICA Japan International Cooperation Agency

KARI Korean Aerospace Research Institute

LOS Line-of-sight

MSL Mean Sea Level

NASA National Aeronautics & Space Administration (USA)

PSCs Permanent Scatterers candidates

PS-InSAR Persistent Scatterer Interferometry Synthetic Aperture Radar

RADAR Radio Detection and Ranging

RCM RADARSAT Constellation Mission

RGB Red-Green-Blue

RSQ R-Squared

RTSD Royal Thai Survey Department

SALT Satellite Altimeter

SAR Synthetic Aperture Radar

SB/SBAS Small Baseline

SCGI Sirindhorn Center of Geo-Informatics

SLC Single-Look Complex

SM Strip Map

SRTM Shuttle Radar Topography Mission

StaMPS-MTI Stanford Method for Persistent Scatterers - Multi-Temporal InSAR

TOP Terrain Observation with Progressive Scans

VV Vertical-Vertical Polarization

WV Wave

1 INTRODUCTION

The flat deltaic-marine Bangkok plain, which is located close to the Gulf of Thailand has heights ranging from 0.5 to 1.5 meters above mean sea level (MSL). This area is underlaid by marine clay known as Bangkok clay (Cox, 1968). This capital city has been affected by land subsidence since early 1970 (Brand & Balasubramaniam, 1976; Inc., 1970; Nutalaya, Chandra, & Balasubramaniam, 1984) and under a continuous threat of flooding and saltwater intrusion because of this area adjacent to the river and into the ocean. The Royal Thai Survey Department (RTSD) had a project to the monitoring of surface subsidence by using leveling benchmarks in the late 1970s. Between 1978 to 1981, the rate of Bangkok metropolitan subsidence area was 10 cm/year in the eastern suburbs and 5-10 cm/year in central Bangkok (David, G. Zeitoun and Eliyahu, 2013). Furthermore, the decrease in the rate of subsidence was 35 mm/year between 1985 and 1988 and 30 mm/year between 1988 and 1991(Phien-wej, Giao, & Nutalaya, 2006). The Japan International Cooperation Agency studied the management of groundwater and land subsidence in the Bangkok Metropolitan area and its vicinity ((JICA), 1995). Besides, over the past fifteen years, the Department of Mineral Resources (DMR), Department of Groundwater Resources (DGR), and Department of Royal Thai Survey have a policy to monitoring land subsidence in Thailand.

However, subsidence and/or compaction of the Quaternary sediment on the Earth's surface deformation response to groundwater over-exploitation, aquifer structure, crustal deformation, active faults, urban construction, land uses types and soil thickness. These different factors have similar effects on the urban area and a subsequent hazardous effect more and more. Consequently, space-based observation on understanding and responding to land subsidence in Bangkok and its vicinity area. Therefore, this study aims to apply the PS-InSAR time-series techniques (A. Ferretti, Prati, & Rocca, 2001; A. J. Hooper, Segall, & Zebker, 2007), to investigate and measure the land subsidence of Bangkok using the Sentinel-1 satellite data between 2016-2019. At the same time, this thesis composes validation data between PS-InSAR and leveling results and decomposing the vertical velocity of PS-InSAR from ascending and descending orbit also.

1.1 Problem Statement

Bangkok is the most economic and social growing city in Thailand with a rapid expansion of the urban area. The development of this urban area could aggravate land subsidence problem, particularly where groundwater usage, transportation construction, sewage, housing or construction buildings, and waste disposal are not well managed. Also, the geological setting of Bangkok mainly consists of clay sequences, from top to bottom as followed; the soft marine clay is an average thickness of about 14 meters, and the stratum of stiff clay is generally thick approximately 5 meters beneath the central Bangkok on the Quaternary basin (Nutalaya et al., 1984). With the progressively growing demand, thus, this area will be damaged by flooding, subsidence, and saline water intrusion. Besides, the rising of global mean sea level driven by climate change affects coastal flooding into low land in Bangkok (Kulp & Strauss, 2019).

There are two possible main factors causing land subsidence in Bangkok and its vicinity area. First of the critical direct factor-induced to land subsidence in the urban area is a growth of population, and consequently the town expansion. Second of indirect by nature factor is geology, hydrology, and/or man-induce causes even though this path seems unimportant, but it has to cause subsidence. Hence, both factors affect land subsidence, which leads to damage in construction and everything on land.

Therefore, measuring and monitoring land subsidence is very important because the evaluation of the velocity of land deformation will help us understand the behaviour of both factors for managing future problems. Presently, space-borne instrument technology is extensive and interesting for scientists worldwide. The Persistent Scatterer Interferometry Synthetic Aperture Radar (PS-InSAR) techniques can detect surface deformation in tropical zones in Thailand.

1.2 Research Motivation

The space-borne Synthetic Aperture Radar (SAR) sensor can detect the structural deformation of the Earth’s surface and can evaluate the SAR image in a

large area. This active sensing technique provides all-day and all-weather mapping capability of considerably high spatial resolution. The SAR data will contribute to mitigating the growing risk of an increasingly urbanized population exposed to such hazards that methods are benefiting to using for the scientific study of the monitoring or measuring land subsidence. We consider the PS-InSAR technique because this methodology can detect ground displacements such as land subsidence, landslide, and earthquake with relatively high precision.

Using Europe's Sentinel-1 spacecraft data, it is possible to generate an interferogram within showing the ground displacements and velocity of movement, including the ability to monitor the dynamic of Earth's surface movement such as ground subsidence, landslide, volcanoes, and glacier flow. The European Commission's Sentinel-1A constellation launch the first satellite on 3 April 2014. The Sentinel-1 radar satellite open-data is systematically and frequently over all the dynamics of a variety of hazard phenomena on Earth. Additionally, the prominent point of C-band sentinel-1 is suitable to detect the change in the urban area.

The persistent scatterer points are complementary distribution on a spatial resolution with millimeter-level accuracy covering enormous on an urban area. The more densely points from the PS-InSAR time-series techniques can preliminary analysis factor of geological relate to land subsidence and represent the land subsidence trend for estimation of the risk subsidence area by statistics method in the future. Nevertheless, we validate the velocity of both orbits with leveling surveys to substantiate the subsidence rate for valuable practice.

1.3 Research Questions and Objectives

The reason why this research considers the scientific question and intends to answer the research question: What and How do PS-InSAR time-series techniques can measure the land subsidence rate (mm/year) in Bangkok by Sentinel-1 satellite image? These techniques achieve by showing the relative velocity (mm/year) and vertical movement (mm/year) of land subsidence in Bangkok and the surrounding area. What are the main factors of subsidence that influence/induce at Bangkok

subsidence? This question can correlate analysis of the geological subsidence from a spatial pattern of the PS-InSAR time-series. The following specific objective:

- To measure the land subsidence rate (mm/year) in Bangkok using PS-InSAR Time-series Techniques.
- To a comparative analysis of the subsidence's descending orbit in the Western Greater Bangkok.
- To validate the relative movement between descending PS-InSAR results and the leveling survey technique in the study area.
- To evaluate the performance of sentinel-1 PS-InSAR Time-series techniques.

1.4 Contribution of the Dissertation

The aim is to use remote sensing data also passive and active, geographic information technology, new technologies, and techniques, as well as find out the result of the questions and objectives of this research. This dissertation is composed of six chapters. The first chapter introduces the research topic by giving a problem statement, explaining the motivation of the research, and the scientific questions and objectives of the research. Research background included land subsidence in Thailand, Thon Buri Basin in the Lower Central Plain or flat deltaic-marine Bangkok plains such as geomorphology-geology-geological structure in Quaternary Basin's Bangkok and hydrology-aquifer system-sea level in the study area, the ESA's Sentinel Mission, reviews of basic Interferometric Synthetic Aperture Radar (InSAR) technique, and PS-InSAR time series present in the second chapter. Chapter III provides the study area and dataset including Sentinel-1 data, benchmark's leveling measurement of RTSD, and methodology workflow of PS-InSAR time-series technique as well as the vertical velocity of PS-InSAR by combined and decomposed the different orbit of PS-InSAR analysis. Result and analysis in Chapter IV present the PS-InSAR time series analysis and validation with leveling survey. The discussions among the validation result, evaluation of the performance of the Sentinel-1 PS-InSAR time-series techniques, limitation of PS-InSAR time-series

techniques, and formation of recent vertical subsidence in Chapter V. The last Chapter VI is conclusions and recommendations in order to succinct summarize the research result and analysis as well as suggests for the future work also.

2 RESEARCH BACKGROUND

The land subsidence in Thailand separated into natural causes and man-induced causes. The natural causes are mainly geological causes, such as quaternary sediment, tectonic setting, and topography. The man-induced causes are mostly groundwater pumping. Also, loads of buildings are an important cause of consolidation in urban areas. As reported since 1978 in DMR, DGR, and RTSD, the cause of subsidence in Bangkok and the surrounding area have three problems; 1) 69% by groundwater over-exploitation 2) 29% by a load of construction and 3) 2% by nature (DGR, 2009).

2.1 Land Subsidence in Thailand

Bangkok's capital city and urban area in Thailand are a high-density population that has been affected by land subsidence since early 1970. The land subsidence problem in Bangkok occurs by groundwater over-exploitation because the water in the aquifer cannot immediately restore in the original state. Therefore, monitoring land subsidence in Thailand is necessary by new technology such as (Aobpaet, 2012; Chaithavee, 2015; Piromthong, 2015). In order to investigate the ground surface deformation in the long-term period, the InSAR techniques are employed in the previous research and as shown in Table 1, which is one method of measuring land subsidence by difference SAR satellite (Figure 1) images.

(Piromthong, 2015) The 10,000 sq.km area in Greater Bangkok was studied the time-series InSAR technique. 18 ERS1 and ERS2 images were covering the period from February 1996 to January 2000. The objectives are to monitor subsidence rate in Greater Bangkok using StaMPS-MTI SB Time-series InSAR techniques on 1996-2000, to validate subsidence rate between GNSS of RTSD and InSAR result and to analysis and combine another thesis (Aobpaet, 2012; Chaithavee, 2015) for finding velocity rate and accumulative subsidence in 1996-2012. The combining result of previous InSAR time-series research during 2005-2010 and 2009-2012. On the other hand, the limitation is phase unwrapping error and double bounce, which did not harmonize with some point result of InSAR and GNSS.

(Aobpaet, 2012) Land subsidence occurring in Bangkok and surrounding provinces by using InSAR, which can accurately measure the earth's surface deformation. The objectives are to apply a combination of specific methods of InSAR (PS and SBAS) to measure occurring subsidence, evaluation of the performance of this technique to monitor, and evaluation of the potentialities and benefits of InSAR. Using 19 images of Radarsat-1 cover most of Bangkok and specific areas of Nonthaburi, Pathumthani, and Samutprakarn for the period October 2005 until March 2010. Also, the InSAR rates are slower can be explained by the phase unwrapping problem, and InSAR has a limitation, but this could be utilized as a geodetic.

(Chaithavee, 2015) The 1600 sq.km area of Greater Bangkok on the east side of Chao Praya river was studied by time-series InSAR Technique. 26 TerraSAR-X images covered the period of September 2009 to August 2012 yields about 2300 scatterers/sq.km. The aims are to monitor subsidence rate in eastern greater Bangkok using time-series InSAR techniques on 2009-2012, to find the trend of study area on 2005-2012 by combine between this result and the thesis result of (Aobpaet, 2012) by RADARSAT-1 and to find a relationship between subsidence rate of InSAR and groundwater level rate. The strength is the high density of the scatterer point because of a high-resolution satellite image (X band). The limitation is similar to (Piromthong, 2015).

The three previous space-based InSAR research, covering almost in Bangkok, studied the same InSAR techniques using the Persistent Scatterer method combine with the Small Baseline method that is different in this research because it is only the Persistent Scatterer method. All antecedent research, including this study, use different acquisition period, different SAR satellite, and different amount of SAR images. Moreover, the validation between InSAR data and leveling benchmarks or GPS stations, confirmed by statistical test (t-test) of land subsidence rate. So, the land subsidence rate by specific InSAR time-series technique can utilize as a geodetic tool to measure and monitor ground surface movement on the Earth. (Chaithavee, 2015) showed a high density of permanent scatterers that related to the high resolution of X-band TerraSAR. (Piromthong, 2015), (Aobpaet, 2012), and (Chaithavee, 2015) found some results of the InSAR area disharmonized with the geodetic station because the

limitation of InSAR analysis is a double-bounce of radar echo and the unwrapped phase error.

Table 1 Previous InSAR studies on land subsidence in Bangkok and its vicinity area

Period Time	SAR Data	Studies	Techniques	Correlation Analysis
Feb 1996 - Jan 2000	18 images ERS1 & ERS2 (C-band)	P. Piromthong, 2015 (Piromthong, 2015)	Combined PS and SBAS Time series	Groundwater
Oct 2005 - Mar 2010	19 images Radarsat-1 (C-band)	A. Aobpate, 2012 (Aobpaet, 2012)	Combined PS and SBAS Time series	Differential settlement and Groundwater
Sep 2009 - Aug 2012	26 images TerraSAR-X (X-band)	S. Chaithavee, 2015 (Chaithavee, 2015)	Combined PS and SBAS Time series	Groundwater
Jan 2016 - 2019	**80 images ASC 93 images DES Sentinel-1 (C-band)**	**This study**	**PS-InSAR Time series**	**Geological subsidence**

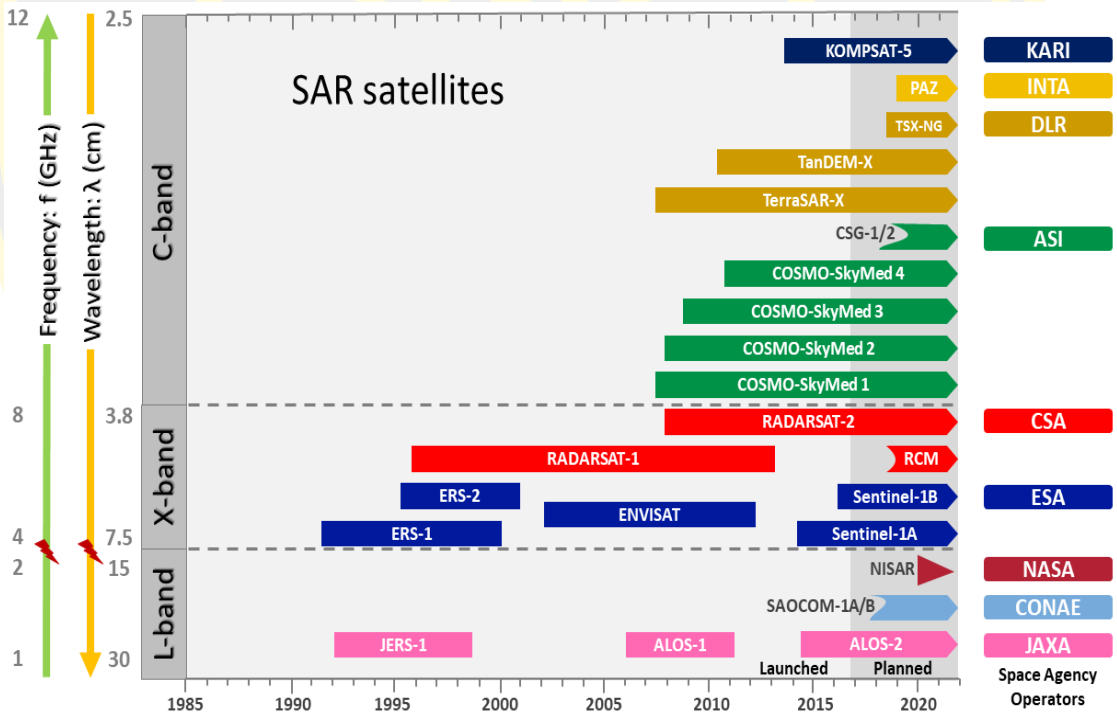

Figure 1 The mission timeline of difference SAR satellites. (modified (Elliott, Walters, & Wright, 2016))

Additionally, the RTSD observed and monitored the land subsidence by first-order leveling technique more than forty years ago (Satirapod, 2020), while in 2006-2018, the result exhibits the subsidence rate is averaging less than 10 millimeters per year in Bangkok and vicinity area. In 2006-2012 as shown as Figure 2 (right map),

almost the leveling benchmark displayed the land subsidence rate is averaging 1 cm/year, but a single point of leveling survey shows the high subsides rate approximately 20 to 30 mm/year in Mueang Samut Sakhon District, Samut Sakhon province that is closed to the Gulf of Thailand and situated on the Tha Chin river of the Lower Central Plain. Every point of leveling benchmark surveying exhibits the land subsidence rate less than 10 mm/year from 2012 to 2018, as seen in Figure 2 (left map), excepting the leveling point in Mueang Samut Sakhon show about 10-20 mm/year. In Bangkok, the decreasing land subsidence rate is a good result of leveling technique. Moreover, this in accord with the result of vertical motion of continuous global position system is 2 millimeter per year as shown as Figure 3. While; the sea level rise is approximately 4-5 mm/year from the multi-satellite altimeter (SALT) and a tide gauge data (Trisirisatayawong, Naeije, Simons, & Fenoglio-Marc, 2011). Also, the flat deltaic-marine Bangkok plain situated in a main four river, average height is close to sea level caused by rising sea levels due to global climate change (GEO2TECDI-SONG, 2013). Therefore, the difference technique study the land subsidence is prevention the subsequent hazardous effect because Bangkok and other provinces are close to the Gulf of Thailand and control the soft clay on the Quaternary basin.

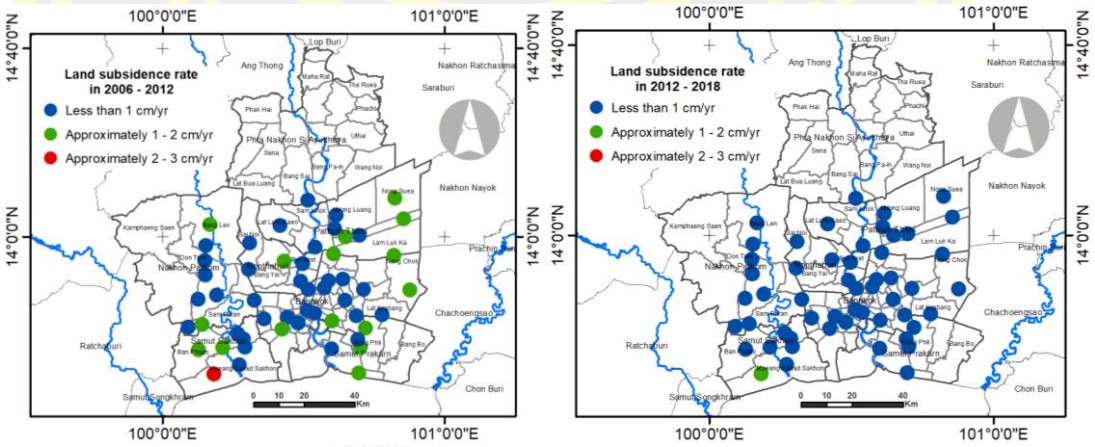

Figure 2 The land subsidence rate in 2006-2012 (right map) and 2012-2018 (left map) by first-order leveling survey technique by RTSD. (credit: Soravis Supavetch) (Satirapod, 2020)

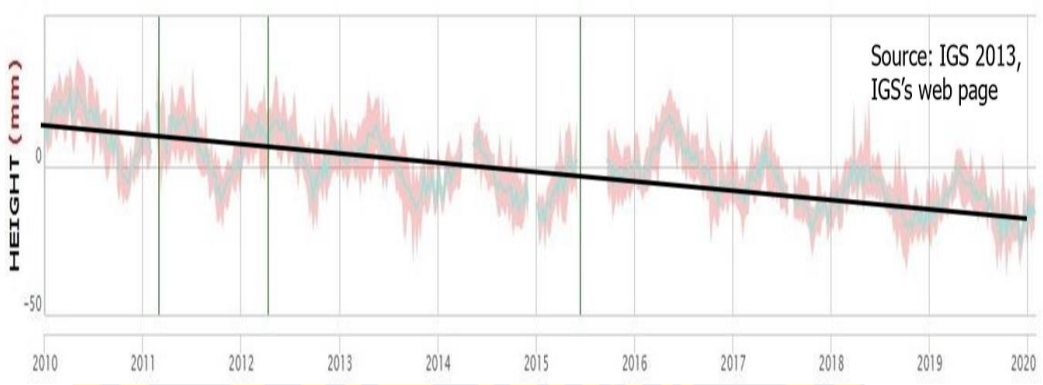

Figure 3 Vertical motion of Continuous Global Positioning System (CGPS) in Bangkok 2010-2020 (Satirapod, 2020).

2.2 Thon Buri Basin in the Lower Central Plain

Bangkok is located in the Thon Buri Basin at the southernmost part of the Lower Central Plain as Figure 4 (Morley, 2015). There are four main rivers (Mae Klong river, Tha Chin river, Cho Phaya river, and Bang Pakong river) run over the area to the Gulf of Thailand. In regional, the Thon Buri Basin is structurally controlled by the NW- to E-S- trending Three Pagodas Fault Zone (Morley, 2015; Searle & Morley, 2019). The schematic cross-section of the Thon Buri Basin is shown in Figure 5. Geomorphologically, the Thon Buri Basin consists of the following landforms: mountain, hill, middle terrace, high terrace, old and young alluvial fans, delta, tidal flat, and flood plain. It has the highest point at Chainat province, the eastern basin margin is close to Lopburi, Saraburi, Nakhon Nayok, Pachinburi and Sachengsao provinces, and the western basin margin close to Uthaitani, Kanjanaburi, and Ratchaburi provinces. In Figure 6 and Figure 7, the yellow colour area represents the extension of soft marine clay or Bangkok clay deposited in the Holocene epoch of the Quaternary period. This sediment layer underlays Phra Nakhon Si Ayutthaya, Suphanburi, Nakhon Nayok, Pathum Thani, Nonthaburi, Bangkok, Nakhon Pathom, Samut Sakhon and Samut Prakarn provinces where the fluvial depositional environment has been interchanged with the shallow marine environment during the Holocene epoch to Present-day.

The southern part of Chao Phaya river (0-4 m above MSL) and the Angthong, Singburi, and Chinat provinces (5-20 m above MSL) are located in the floodplain areas. The western and eastern geomorphology is characterized by low terraces that have elevation above mean sea level between 5-45 m. In Figure 5, the blue colour represents high terraces, and green colour represents hard rock, which forms the basin margin in Bangkok. The general geomorphology of Bangkok plain is controlled by floodplain deposits environment in Holocene that was underlaid by Bangkok clay-like low-swelling of the intrinsic (physical, permeability, and compressibility) clay (Horpibulsuk, Yangsukkaseam, Chinkulkijniwat, & Du, 2011).

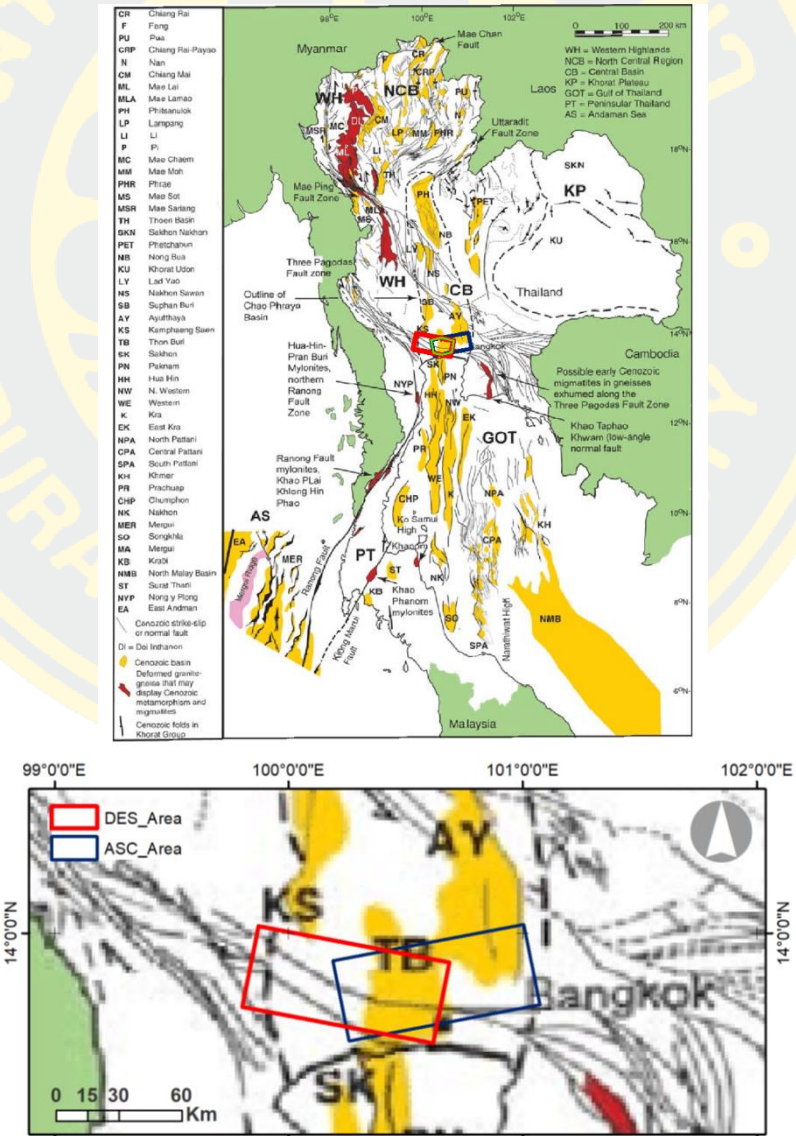

Figure 4 The ASC and DES study area on the Thon Buri Basin located Thailand's Cenozoic structural features and basins map (created by (Morley, 2015)).

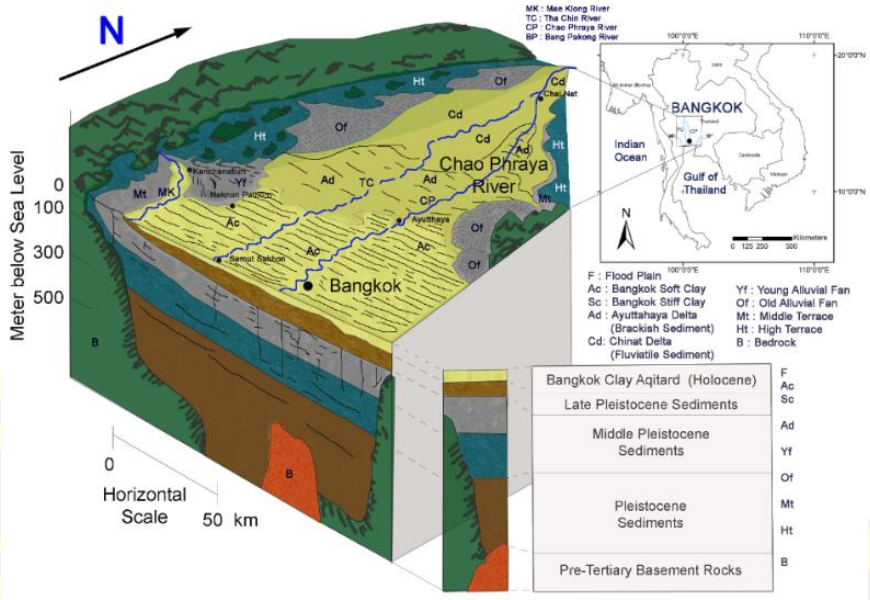

Figure 5 Cross-section of the Thon Buri Basin situated the lower central plain (Modified ((JICA), 1995))

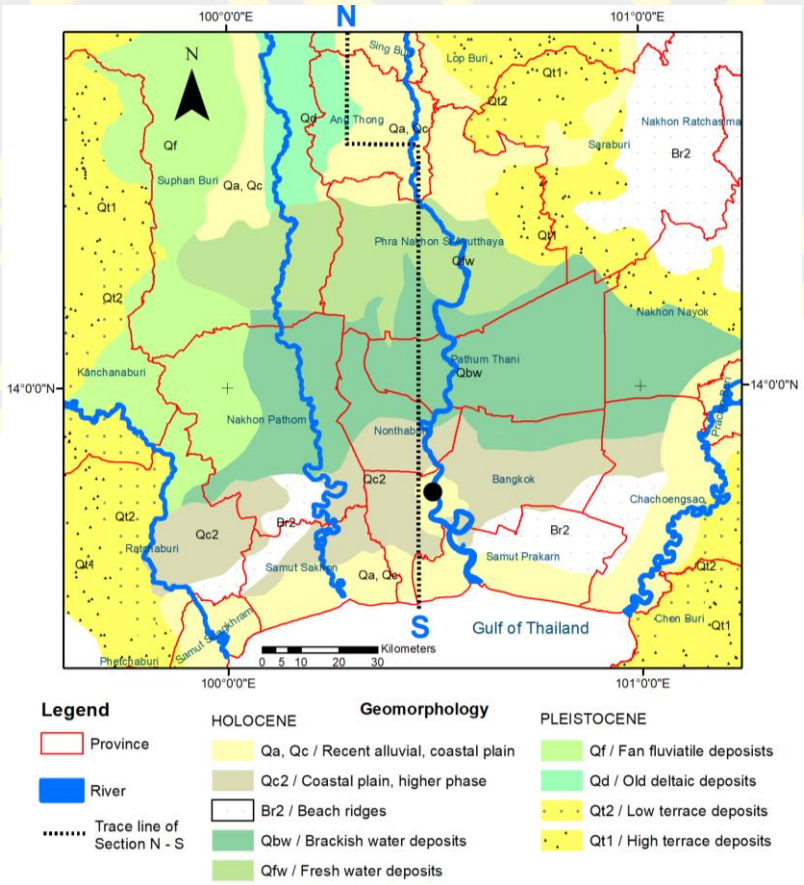

Figure 6 Geomorphology and Geology map in the Quaternary basin's Bangkok (DGR, 2012).

According to Figure 5 and Figure 6, the fluvial and marine depositional environment in the Bangkok can be explained as follows: The lower Pleistocene epoch has Qt1 (the layer of sand, gravel-silt, and large laterite layer from bottom to top) of the high terrace (Pliocene-Early Pleistocene) and Ot2 (clay silt sand gravel covered by thin laterite layer in a ridge of the basin. The upper Pleistocene epoch has Qd in fan fluviatile deposit and Qf in an old deltaic deposit. The lower Holocene epoch has sand and silt in fresh and brackish water deposits (Qfw and Qtw) while the upper of the Holocene epoch has a dark grey to black clay marine deposit (Br2, Qc2, Qc, and Qa). The NS line, as shown in Figure 6, can explain the geological cross-section of the aquifer system in the Bangkok area in Figure 7. Bangkok clay consists of soft clay overlying stiff clay, sand, gravel, and clay constitute the principal aquifers of Bangkok. The aquifers are as follows: Bangkok aquifer, Phra Pradaeng aquifer, Nakorn Luang aquifer, Nonthaburi aquifer, Sam Khok aquifer, Phraya Thai aquifer, Thon Buri aquifer, and Pak Nam aquifer as shown in Figure 7.

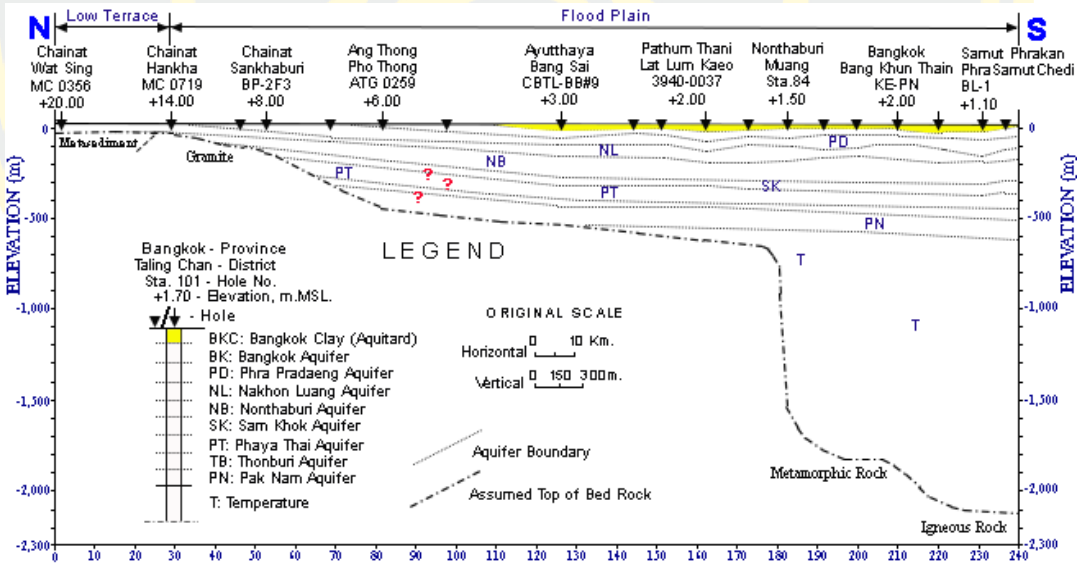

Figure 7 A geological cross-section of the aquifer system in the Bangkok area ((JICA), 1995; DGR, 2012).

Bangkok city consists of unconsolidated sediments as clay, silt, peat, and sand that are particularly susceptible to surface subsidence (David, 2013). Three different land subsidence types probably occurred in Basin's Bangkok and the surrounding area: locally subsidence due to groundwater extraction, compaction subsidence

induced by a load of construction, regional subsidence caused by the thermal subsidence of the Thon Buri Basin since the Late Miocene (Morley, 2015). On the whole, every phenomena type of land subsidence can occur in the Quaternary Basin's Bangkok clay that consists of soft marine clay, 15 m to 30 m in thickness. The DMR identified and named eight aquifers by logs of groundwater wells. These aquifers consist mainly of sand and gravel separated by clay beds. The stratigraphic sequence in the Lower Central Plain, the Bangkok clay, is the most important unit in terms of land subsidence (Sinsakul, 2000).

2.3 ESA's Sentinel-1 Mission

The Sentinel-1 satellite Earth Observation system has made systematic, large-area observations possible, that are useful for monitoring Earth's surface movement. This satellite is in sun-synchronous low-earth orbits along with a typical 600–800 km altitude with periods of 95–100 min. Besides, the ESA's mission has an open-data policy. This data policy was opened to everyone for downloading the Sentinel data on the scientific hub: http://scihub.copernicus.eu/ since on 3 October 2014, which will ensure that this is the fundamental tool for measuring deformation at small over large areas on Earth's surface. The Sentinel-1 data consists of a C-band SAR instrument (5.405 GHz), which has a wavelength of 5.547 cm. This data has four exclusive imaging modes (Stripmap (SM), Interferometric Wide Swath (IW), Extra-Wide swath (EW), Wave (WV)). The European Commission's Sentinel-1 constellation launch (Figure 1) the first Sentinel-1A satellite on 3 April 2014, revisit periods of 12 days, and the second Sentinel-1B on 25 April 2016, revisit periods of 6 days.

The Sentinel-1A radar satellite administrated by the ESA as a part of the Global Monitoring for Environment and Security (GMES) Space Component Programme (Elliott et al., 2016; Snoeij et al., 2010; Torres et al., 2012). The Sentinel data is systematically and frequently over all the dynamics of a variety of geophysical phenomena on the Earth. The short period of revisit time and a small orbital baseline is a significant advancement because it enabled interferograms better maintain coherence and capture time-dependent deformation. So, providing a more significant number of sampling observations is simply to reduce atmospheric noise in measuring

small displacement accumulation or surface deformation (e.g., tectonics movement and land subsidence) and dynamic of the cryosphere. Additionally, the Sentinel-1 mission focuses on working applications such as the land surface mapping including a cover of vegetation (e.g., forest) and crises mappings, such as natural disasters (e.g., earthquakes and flooding phenomena) and humanitarian aid, as well as the observation of the marine environment, including oil spill detection and monitoring the sea-ice in Arctic or Antarctic, the maritime transport surveillance.

2.4 InSAR Techniques for the Estimation of Surface Displacements

Radar Remote Sensing is active remote sensing that can collect data by RADAR sensor operate within the electromagnetic spectrum of microwave (1mm-1m) also can be used to support studying and measuring the surface movement. Additionally, but also penetrated and detected to object under almost weather, SAR can use long time-series data in the area of interest. Due to radar image or SAR image, is consists of the amplitude and the phase. The amplitude can be analyzed the scattering properties on the surface of the Earth (A. Hooper, Bekaert, Spaans, & Arikan, 2012) or backscattering intensity on SAR images (Balz, 2019), as shown in Figure 8. This figure interpreted the mean amplitude map, can three-backscattering classes by primitive form. Viz very bright backscattering (white colour) represents like the metal-perpendicular style structures as well as the human-made objects, and very low backscattering (back colour) such as undisturbed water surfaces, roads. On the other hand, the phase represents a distance between the radar sensor to the object, as shown in Figure 9(a).

Interferometric synthetic aperture radar (InSAR) uses the phase difference that can be interpreted surface displacement or in terms of the changes in LOS from between two coherent radar signals as a difference in distance between two acquisitions (Balz, 2019). Interferometric SAR is a technique involving different phase measurements (Figure 9(a), Eq 1, and Eq 2) from transmitted-received system satellite SAR data to detect very slight changes on the Earth's surface with high accuracy scale and reliability. Besides, SAR interferometry is a crucial technology based on two components on every pixel as amplitude is a representation of the

intensity of backscattering, and phase represents the distance between the sensor and object. Both components on a pixel are vector result of backscattering by scatterers.

Measuring ground deformation by InSAR is an advantageous technique along with deriving reliable source parameters and high-resolution models for land subsidence. SAR interferometry has been demonstrated successfully in several applications, including topographic mapping, measuring and monitoring land subsidence (Figure 9(b)), measuring displacement as a result of landslide or earthquakes, and flow rates measurement of large ice sheets or glaciers. The InSAR system can record the phase difference of SAR image at a different time in the same object point that the phase difference is changed ground surface deformation, as explained in Figure 9(a). The urban area has a high density of buildings that is a stable object. For this reason, the PS-InSAR time-series technique is suitable for measuring the movement of the object on the Earth's surface, as shown in Figure 10.

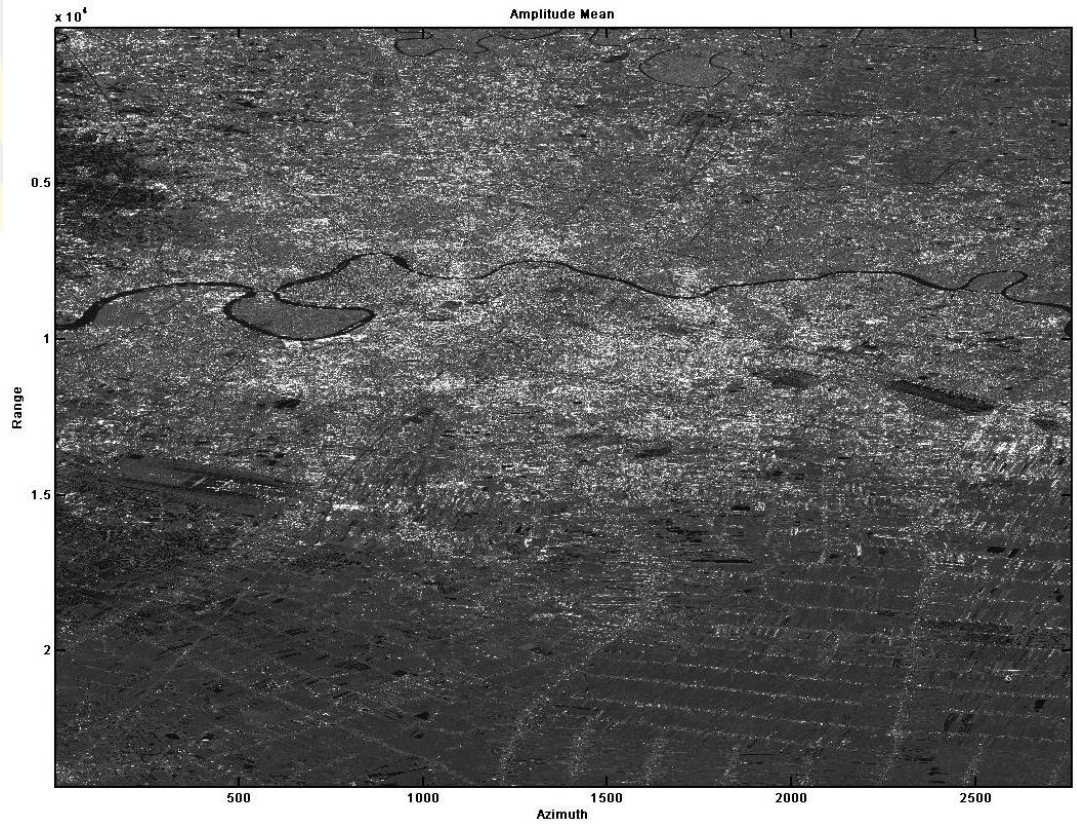

Figure 8 The mean of the amplitude map in ascending orbit using PS-InSAR techniques by SARPROZ software. (The grey colours range represents a backscattering strength.)

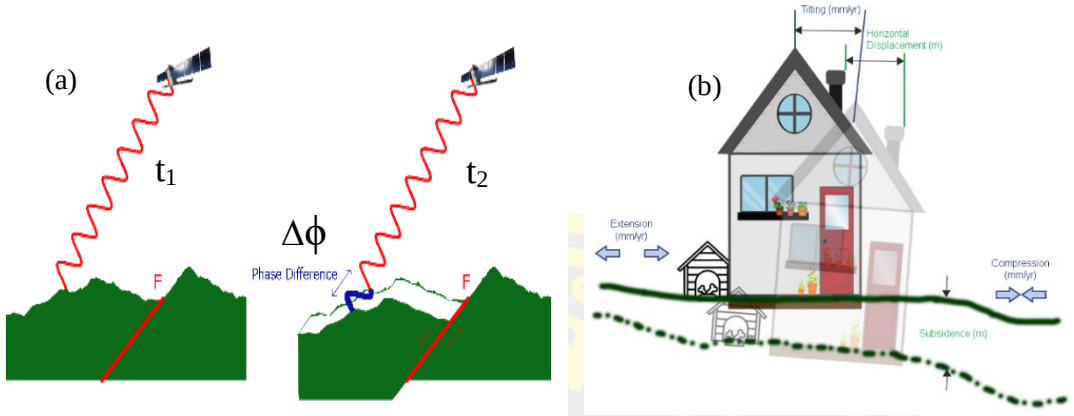

Figure 9 (a) Schematic illustration explaining the repeat pass interferometry. (b) Movement of objects due to surface deformation. (modified (Eckardt et al., 2019))

2.4.1 PS-InSAR Time-Series

Permanent Scatterer (PS) InSAR (A. Ferretti et al., 2001) time-series process is a special form of differential interferometry (Figure 12 and Figure 13). It uses many pair interferometry radar images, combined into a long time series. According to Figure 10, the strong dominant scatterer, such as a building, rock, bridges, well-known persistent scatterer pixels, is characteristic scattering to remaining stable and containing a single point scatterer. This figure presents two cases, as distributed scatterer pixel (left image) and persistent scatterer pixel (right image). The aim of PS-InSAR, the identification of stable scatterers that their backscatter properties are similar in every image acquisition for detection slow surface motions, and also allows measuring of small-displacement, through the error sources reduction (A. Hooper et al., 2012). So, the PS-InSAR is possible to create map ground surface deformation based on phase differences images, as seen in Equation 1. This technique measures the ground deformation on a scale of millimeters in the line of sight (range) of the radar.

The first common to achieve precise measuring deformation of Earth's surface or other crustal deformation phenomena, whereby high-quality indicator from SAR Interferometry, is a good coherence base on the similarity between the images (Balz, 2019). Both main interferometric error sources due to temporal in InSAR are the decorrelation of geometric effects and phase error (Simons & Rosen, 2015). However, the interferometric SAR has powerfully affected the atmospheric delay in the

troposphere and ionosphere. In addition to orbit error, topographic effect and decorrelation noise are factors to reduces decorrelation, as shown in Equation 2, for finding the phase contribution related to ground deformation.

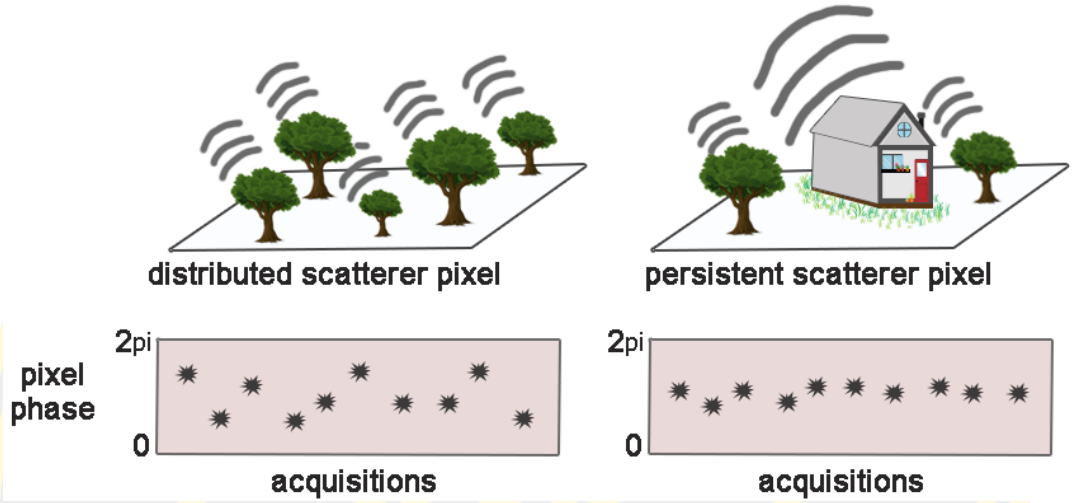

Figure 10 Concept of Persistent Scatterer Interferometry of distributed scatterer pixel (left image) and persistent scatterer pixel on the right side of the figure.

2.4.2 Equation

The SAR system is transmitting the pulse that consists of phase and amplitude. So, the phase difference represents the Earth's surface movement by using the phase difference between two SAR acquisitions ($\Delta\phi$), as shown in Equation 1. Hence, $\Delta\phi$ can calculate the ground surface movement in LOS of a satellite (Δr), but $\Delta\phi$ is wrapped difference phase form. So, measuring the deformation, the interferometric phase needs to be unwrapped. Simultaneously, the fundamental InSAR principle is used differential SAR interferometry (DInSAR) by a spatial ground surface of a stable object. The phase difference ($\Delta\phi$) (A. Ferretti et al., 2001; Hanssen, 2001) as shown in Equation 2 is the summation of a phase of surface movement, or phase contribution of the pixel in the satellite LOS direction relate to ground deformation (ϕ_{def}), phase of orbit error (ϕ_{orbit}), topographic effect phase (ϕ_{topo}), phase of noise (ϕ_{noise}), and atmospheric phase delay (ϕ_{atm}). The phase difference is calculated base on Equation 1 and Equation 2:

$$\Delta\phi = \phi_1 - \phi_2 = \frac{4\pi}{\lambda}\Delta r \qquad \text{Equation 1}$$

where

ϕ_1, ϕ_2: the phase of each acquisition

Δr: the difference in range (LOS) between two SAR acquisitions

λ: wavelength of radar

$$\Delta\phi = \phi_{def} + \phi_{orbit} + \phi_{topo} + \phi_{noise} + \phi_{atm} \quad \text{Equation 2}$$

where

$\Delta\phi$: interferometric phase (or phase difference)

ϕ_{def}: phase contribution related to ground deformation

ϕ_{orbit}: Orbit Error

ϕ_{topo}: Topographic Effect

ϕ_{noise}: Noise

ϕ_{atm}: Atmospheric Delay

As shown in Equation 2, the interferometric difference phase is a sum of many phenomena such that errors in satellite position and topography alter deformation measurements. Furthermore, changing atmospheric conditions also degrade the deformation signal. Since 2000, many groups worked on mitigating these unwanted signals, using multiple acquisitions over the same area (Balz, 2019; Berardino, 2002; A. Ferretti, Prati, & Rocca, 2000; A. Ferretti et al., 2001; A. P. Ferretti, C.; Rocca, F., 1999; A. J. Hooper, 2006; A. J. Hooper et al., 2007; Werner, 2003).

3 METHODOLOGY

3.1 Study Area and Data Set

3.1.1 Study area

The 3,450 km^2 of ascending track and 3,450 km^2 of descending track study area, situated in the Quaternary basin (99.804109 E–101.074404 E; 13.529357 N–14.036832 N). The capital of Thailand is located in the Central Plain that stretches from the Gulf of Thailand to as cover Bangkok city also some part of Pathum Thani, Nonthaburi, Samut Sakhon, Samut Prakan, Chachoengsao, Ratchaburi, and Nakhon Pathom provinces in Thailand. The footprint of the scene location can found in Figure 11. This figure was base on a Sentinel-2 background infrared false colour image (Band 8: Red (R), Band 4: Green (G), Band 2: Blue (B)) in December 2019. The false infrared colour of the Sentinel-2 image exhibit construction area in greyish colour, agriculture area in reddish colour, and swamps in greenish colours. The red square footprint background presents the RGB composite of coherence, mean, and difference backscatter by Sentinel-1 between August and October 2019. The yellow-coloured area displays high backscatter and high coherence value in the descending red box. So, the yellow area is an urban area. However, the stable area (e.g., urban area, bare soil) and changing area (forest areas) that are apparent the high coherence and low coherence. The interpretation will observe the backscatter together because the high backscatter/double bounce represents an urban or forest area, but the low backscatter/single bounce is shown a bare soil or agriculture area.

3.1.2 Sentinel-1 data

The Sentinel-1A data with IW2 sub-swath-VV polarization and normal baselines of <150 m and 2016-2019 temporal baseline period, between master and slave images, for the study area. This SLC data in the study area consists of C band images, which have a wavelength of 5.547 cm, Resolution 5x20 meters, Interferometric Wide Swath length 250 km. All images were selected 80 images of the path as 172 between 28/1/2016 and 21/09/2019 of ascending flight direction, as well as 93 images of the path as 62 as between 8/1/2016 and 7/10/2019 of descending flight direction as shown on Table 2. The long length of the radar images series of this

thesis can obtain the higher the accuracy result of velocity measurement (A. Ferretti et al., 2011). SARPROZ software was used for PS-InSAR time-series analysis to derive land surface displacement, relative movement, and combine PS-InSAR analysis from difference orbit.

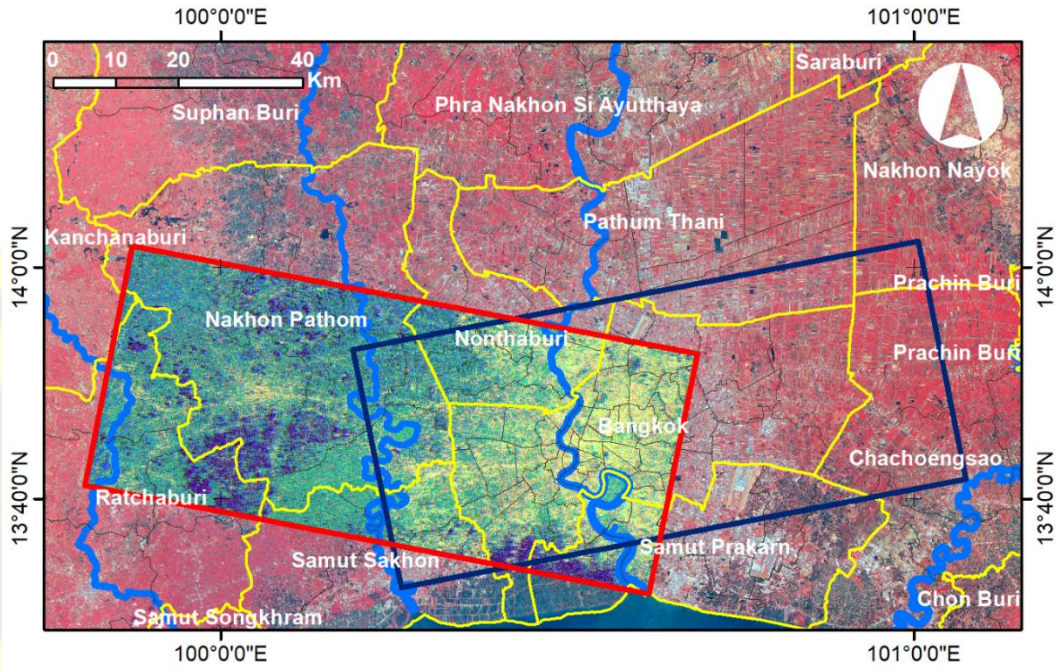

Figure 11 The study area and data set in Thailand. The red and blue square box footprint of Sentinel-1 TOPS-IW2-VV images indicates the descending and ascending orbit in Table 2.

For the descending analysis, 93 scenes were chosen, with the master image in September 2017, while for the ascending analysis, 80 senses were chosen with the master image in June 2017. The ascending data set is a lack of data from January 2017, late September 2019 to early October 2019. So, the date of the ascending master image is earlier than the descending master date. Furthermore, it can be seen in Figure 12 and Figure 13.

Table 2 Properties of the downloaded Sentinel-1 data for both the ascending orbit and descending orbit.

	Ascending (Figure 12)	**Descending (Figure 13)**
Number of scenes	80	93
Acquisition period	2016-Jan-28 to 2019-Sep-21	2016-Jan-08 to 2019-Oct-07
Master image	2017-June-15	2017-September-23
Relative orbit number	172	62
Incidence angle	38.3	
Acquisition mode	Interferometric Wide swath (IW)	
Product level	1	
Product type	Single Look Complex (SLC)	
Polarization	Vertical-Vertical (VV)	

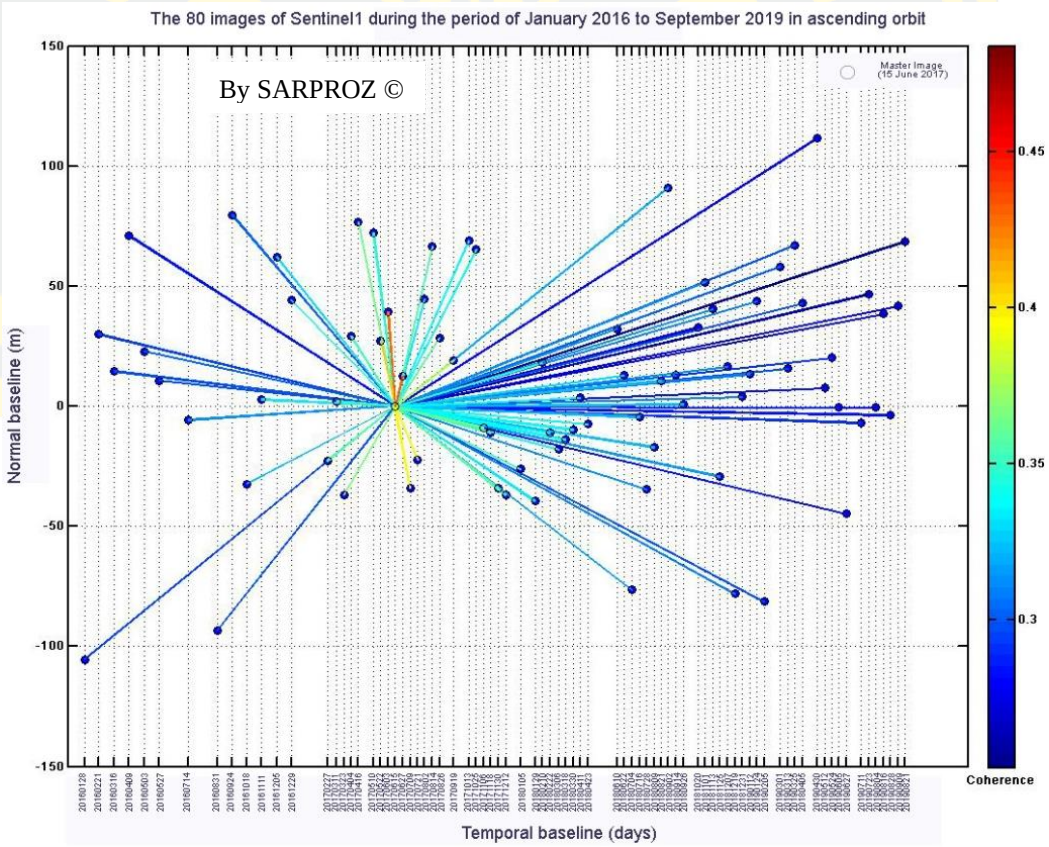

Figure 12 The ascending Sentinel-1 images plot between normal baselines (m) and temporal baselines (days). A white center circle represents Master image, blue circles are Slave images, and lines represent the Interferograms formed between Master and Slave image.

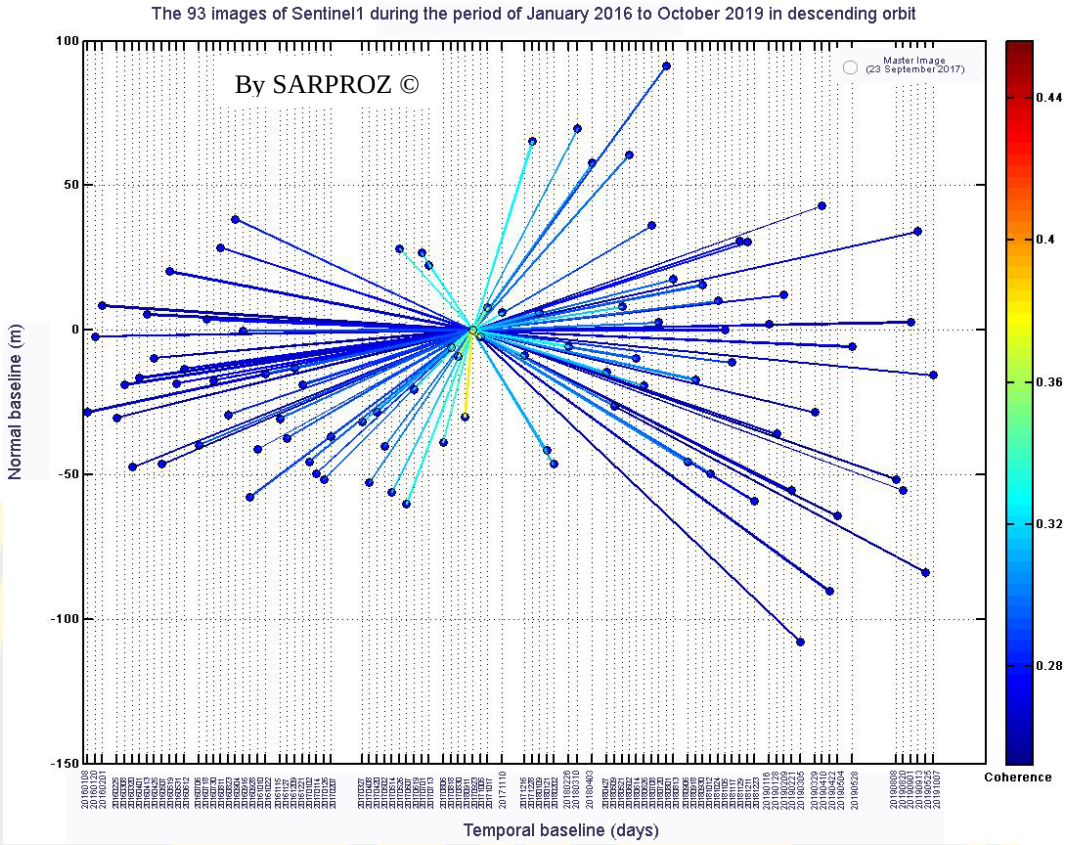

Figure 13 The descending Sentinel-1 images plot between normal baselines (m) and temporal baselines (days). A white center circle represents Master image, blue circles are Slave images, and lines represent the Interferograms formed between Master and Slave image.

3.1.3 Leveling benchmark

The leveling survey is the best basic method for measuring the vertical movement of benchmark in land surface subsidence while InSAR techniques are different criteria in Table 3. However, these two main methods can monitor and accurate measuring of the velocity of movement (mm/year).

Table 3 A short comparison of leveling benchmark and PS-InSAR techniques.

	Sentinel-1 PS-InSAR	**Leveling Benchmark**
Spatial resolution	5x20 m	>250 m
Spatial characteristics	Urban area	Leveling line
Temporal aspects	Data available every 6–46 days (+archived data), processing takes only a few hours or days	Roughly 20–50 benchmarks/day, campaign repeated several times
Human resources	Time series of satellite data, PSI software	Instruments, benchmarks, traveling costs, leveling software
Observation density	>Hundreds/km^2 (built-up area, where PS are available)	Lines, Tens/km^2 (targets can be selected)
Accuracy	<1 cm	1 mm for 1 km of line

In 1978, the Royal Thai Survey Department (RTSD) measured absolute subsidence from the first-order leveling survey in Bangkok. At the same time, the benchmarks are constructed near the groundwater monitoring stations by the Department of Mineral Resources (DMR). Latterly, the leveling benchmark survey expanded to the surrounding area as Pathum Thani, Nonthaburi, Samut Sakhon, Samut Prakan, and Nakhon Pathom province as close to Bangkok by RTSD.

The locations of the 81 leveling points Figure 14 were conducted at more than 20 meters of benchmark depth in sedimentary bed because the benchmark of leveling point harmonize with measuring land subsidence in the study area using the InSAR technique, including as the microwave reflects construction building. In addition, most of the foundation pile drill down the sedimentary bed of depth. The leveling benchmark of RTSD represents difference value in elevation of points concerning a reference point (BKK5127). Consequently, this BBK5127 reference point is precise the leveling, stronger stable point, represents using validation of relative movement between leveling point and PS-InSAR time-series point.

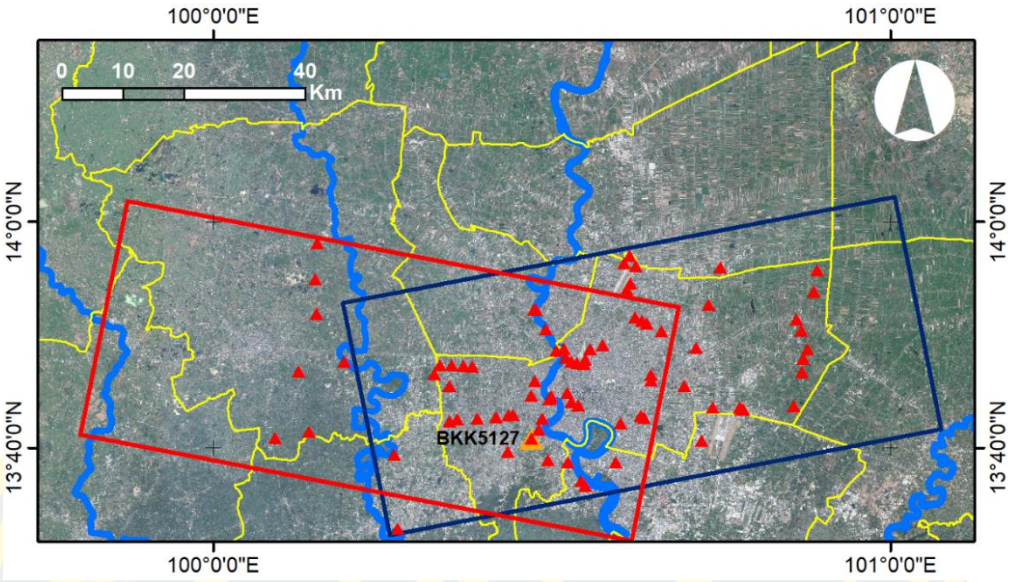

Figure 14 The 81 leveling survey benchmarks in the ascending and descending orbits.

In Figure 14, The red and blue square box footprint indicates the descending and ascending orbits of Sentinel-1 TOPS-IW2-VV images. The orange triangle point is the reference point (BKK5127). The leveling data of four years surveying (2011, 2012, 2016, and 2018) from RTSD will be used to validate the PS-InSAR time series analysis result between early January 2016 to early October 2019 in descending area.

3.2 Methodology Workflow

3.2.1 PS-InSAR time-series technique

The PS-InSAR time-series techniques can detect ground subsidence movement with relatively high precision at millimeter variations in the line-of-sight velocity (Perissin, 2008), take advantage of pixels dominated by a single scatterer to reduce the influence of atmosphere and decorrelation. This technique is to consists of data preparation, pre-processing data, processing (preliminary analysis and geocoding), and InSAR processing, as shown in Figure 15 related to Equation 1 and Equation 2. Furthermore, changing atmospheric conditions also degrade the deformation signal. Aside from these deterministic phase contributions, the unwrapping of the interferometric phase is a non-deterministic problem that has many equally correct solutions, and can only be solved under certain assumptions.

The main objective of this research is to measure land subsidence using PS-InSAR time-series technique form open Sentinel-1 data, as well as validate PS-InSAR point with leveling benchmark surveying of RTSD. The PS-InSAR analyses were administered in the SARPROZ software (Benattou, Balz, & Liao, 2018; Fryksten & Nilfouroushan, 2019; Perissin, 2016; Perissin et al., 2012; Perissin, Wang, & Wang, 2011) (www.sarproz.com). This study is composed of 4 steps, as shown in Figure 15: First, the preparation SLC-IW mode data is download and using a single-master configuration in both orbits. The second, a pre-processing data consists of the selecting TOPS data, read precise orbit, and co-registration for removing the orbit error for the satellite orbit by comparing the images pixel-by-pixel. Thirdly, processing generates the InSAR by using external DEM and GCP selection for extracting the topographic effect. The InSAR processing last part is to eliminate the noise, atmospheric delay, and phase unwrap processing in time-series analysis; as a result, the relative land subsidence. As discussed in more detail below.

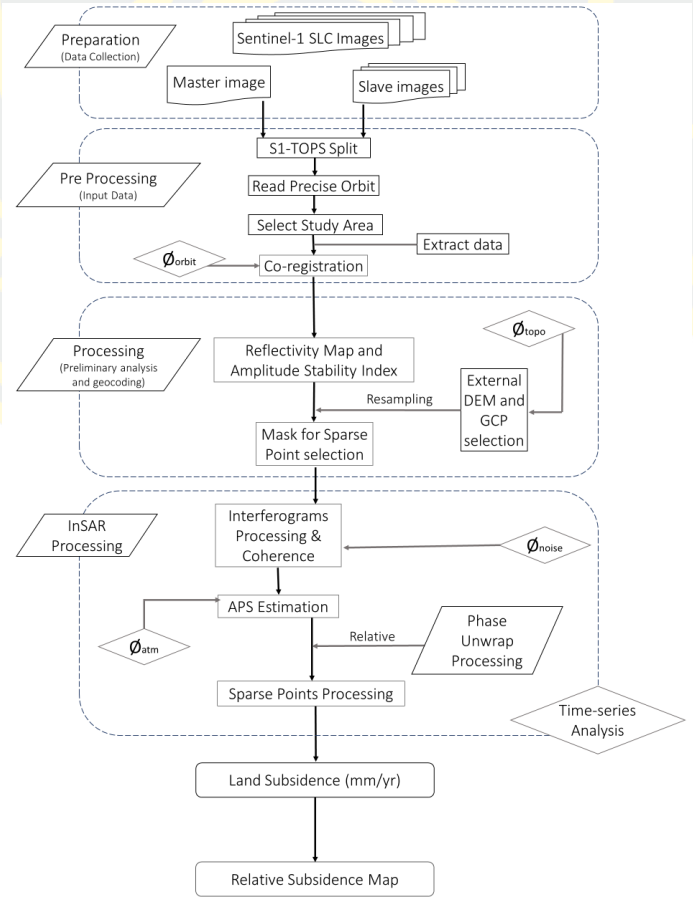

Figure 15 Workflow of PS-InSAR time-series processing in this research.

Data Preparation: This research used the ascending and descending SLC Sentinel-1 data as C-band, can afford high precision in the interferometric processing in the study area. The interferogram occurs between only one mater image and slave images in the all series of the image, as shown in Figure 12 and Figure 13. The suitable pairs of SAR interferometry composed a spatially normal baseline and temporal baseline, whereby the master image is on 15 June 2017 for the ascending dataset and on 23 September 2017 for the descending dataset. The normal baseline of 79 pairs of ascending orbit and 92 pairs of descending orbit are between 0-120 meters while both orbits of the temporal baseline interferometry are between 12-797 days of January 2016 to September 2019 on ascending track and 12-744 days of January 2016 to October 2019 on descending track.

Pre-Processing Data: The Sentinel-1 TOPS data to be selected a VV polarization and IW2 subs with to cover the area of interest, applied precise orbits, then extracted and co-registered the master image and slave images. The co-registration is the process of the SAR data to a common radar coordinate system with geometric precision by calculating the pair of slave images in the geometry of the master image. The scatterers of interferograms in both images are carried out using data from satellite orbit and achieved an accuracy of a pixel (Balz, 2019). The Interferogram is generated by multiplying the complex SAR values of the slave image with the complex conjugate of the corresponding master image (Gupta, 2002).

Processing (Preliminary analysis and geocoding): After the SLC dataset of sentinel-1 were prepared on IW2-VV polarization and the interferogram generated by the co-registration of the master and slave image. The Permanent Scatterers candidates (PSCs) (Kampes, 2006) are selected; as a low the dispersion of amplitude index for each pixel varies in time. The SARPROZ software automatically downloaded the one arc-second SRTM, as well as DEM 30 m, that covered the study area. The removal of the topographic phases uses the external DEM to similarly the flat Earth. When reflectivity map and amplitude stability index had been finished, then these datasets were geocoded in the mask for sparse and ground control point selection process. In ascending dataset and descending dataset had the same ground control point.

InSAR Processing: In this process consists of the interferogram processing, coherence map generation, atmospheric phase screen (APS), and sparse points processing. The aim of the InSAR processing in the last step is to estimate the atmospheric phase and get the final time series of deformation whereby the measuring from permanent scatterers or stable point. This step, also known as the PS-InSAR time-series technique, is a method to search for the pixels that were based on the stable phase and temporal coherence over a long time. All things considered, the reference point as the same as the reference leveling point (BKK5127), that special consideration to select the PS-InSAR reference point (Figure 19) in a relatively stable and close to the BKK5127.

3.2.2 Decompose the Vertical Velocity of PS-InSAR

This processing step considers the decomposed of the vertical velocity on the ground deformation over the entire time interval in both ascending and descending geometry. The deformation along a line-of-sight of ascending orbit and descending orbit for value point datasets (d_{LOSasc} and $d_{LOSdesc}$) as shown in Figure 17 and Figure 18, were concerned the hexagonal area of interest as shown in Figure 30. The mean of d_{LOSasc} and $d_{LOSdesc}$ were derived by created the 25 sq.km grid size square in the interesting hexagon area. Then is found out the average velocity on LOS in the direction of both orbits of each grid-point. This research used the Sentinel-1 IW2 datasets, so all detail of this satellite, as shown in Table 2 and explained in Figure 12(a).

The velocity of the PS-InSAR time-series technique is a real deformation vector on the radar line of sight. So, in the interesting hexagon area, use the Equation 3 and Equation 4 (Fuhrmann & Garthwaite, 2019; Gudmundsson, Sigmundsson, & Carstensen, 2002; Mohamadi, Balz, & Younes, 2019; Pepe, 2007; Pepe & Calò, 2017; Samieie-Esfahany et al., 2010; Schaufler, Bauer-Marschallinger, Hochstöger, & Wagner, 2018; Spata, Guglielmino, Nunnari, & Puglisi, 2009; Wright, Parsons, & Lu, 2004) to compose the vertical motion (d_{vert}) on the land subsidence of the ascending and descending geometries as shown in Figure 16(b).

$$\begin{pmatrix} d_{LOSasc} \\ d_{Losdesc} \end{pmatrix} = \mathbf{A} \begin{pmatrix} d_{Vert} \\ d_{HALD} \end{pmatrix} \quad \text{Equation 3}$$

$$\mathbf{A} = \begin{pmatrix} \cos\theta asc & \frac{\sin\theta asc}{\cos\theta\Delta\alpha} \\ \cos\theta desc & \sin\theta desc \end{pmatrix} \quad \text{Equation 4}$$

where

d_{LOS}: Deformation along a line of sight (LOS)

d_{Vert}: Vertical motion

d_{HALD}: Horizontal in descending ALD

θ: Incidence angle

$\Delta\alpha$: Difference of the heading satellite between ascending and descending orbit

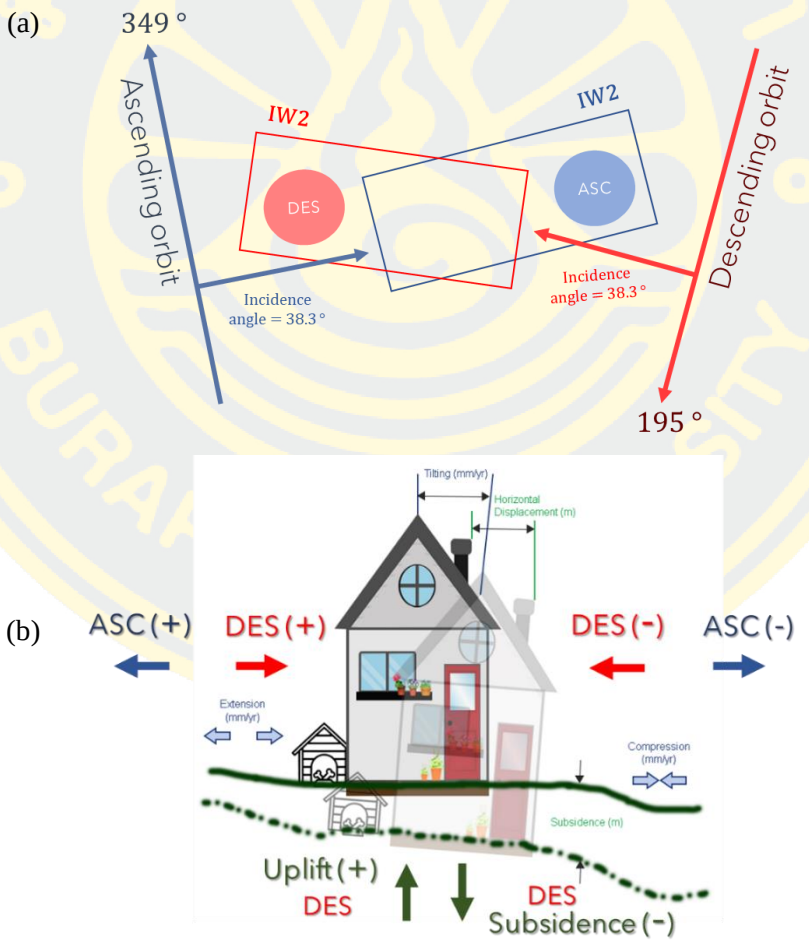

Figure 16 (a) The schematic view of difference azimuth angle the Sentinel-1 acquisition on ascending and descending satellite orbit. (b) Movement of the object due to land surface deformation.

4 RESULT AND ANALYSIS

In this chapter described a result and analysis that demonstrated the relative velocity of stable points by the PS-InSAR Sentinel-1 time-series processing in SARPROZ software. In addition to considering as the subsidence's descending orbit was compared in the Western Greater Bangkok and validated the relative velocity point between PS-InSAR results and the leveling survey technique by RTSD. First of all, the ascending and descending of Sentinel-1 satellite datasets in the SLC level be downloaded from 2016 to 2019 of the European Space Agency's platforms that the detail as seen in Table 3, Figure 12, and Figure 13. After obtaining time-series data, all images of ascending and descending paths be processed that following the method on PS-InSAR time-series technique, as seen in Figure 15. The goal of PS-InSAR time-series techniques is to measure or estimate the land subsidence rate even though this technique can detect several phenomena deformation along the radar line-of-sight direction on the Earth's surface but eliminating the source error or different effects such as orbit error, topographic effect, noise, and atmospheric delay is important. So, The PS-InSAR time-series processing is composing many steps for measuring the velocity of land subsidence in the research area.

4.1 PS-InSAR Time-Series Analysis

The PS-InSAR time series were employed to analyze 80 images of ascending Sentinel-1 dataset from January 2016 to September 2019. The footprint covers some parts of Bangkok, Samut Prakarn, Samut Sakhon, Nonthaburi, Nakhon Pathom, Nakhon Nayok, and Chachoengsao provinces. The 276,774 PS points, yielding the density of 80 points/km^2 detected as a stable point in the ascending area as shown in Figure 17. This area appeared to be compaction slowly at an average rate approximately 4.81 mm/yr. Fast relative velocity subsidence between 8 to 25 mm/yr is found in the northeast of the ascending area located in Pathum Thani, Nakhon Nayok, and Chachoengsao provinces. After obtaining the result in the ascending orbit, Chachoengsao province is an attractive urban area to study land subsidence because this province, including Eastern Economic Corridor province, will be expanding the economy, population, and infrastructure. Also, the Bang Nam Priao district, Chachoengsao province is controlled by residential, agriculture, aquaculture, and

industrial zones. While the high subsidence on Lum Lok Ka district at Pathum Thani province and Ongkharak district at Nakhon Nayok are controlled by industrial and residential zones.

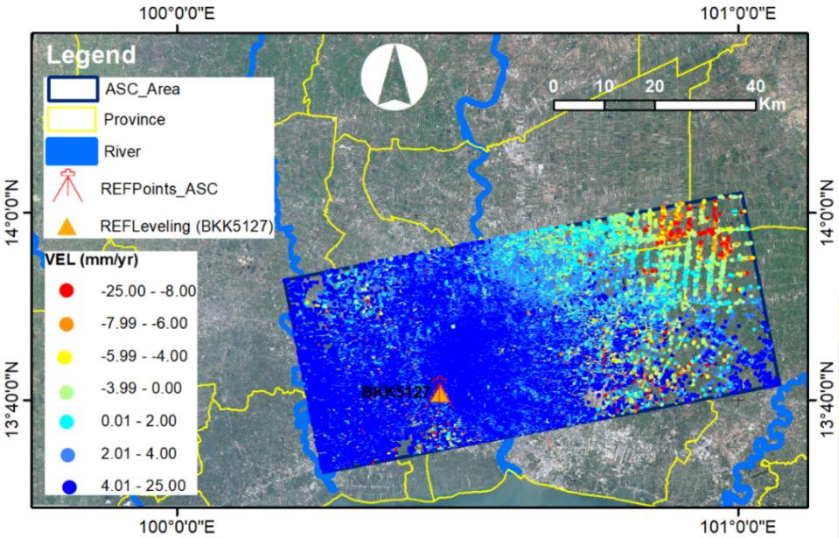

Figure 17 The relative velocity map of the PS-InSAR point from ascending analyses.

The PS-InSAR time series were employed to analyze 93 images of descending Sentinel-1 dataset from January 2016 to October 2019. The footprint covers almost Bangkok and some parts of Samut Prakarn, Samut Sakhon, Nonthaburi, Ratchaburi and Nakhon Pathom provinces. The 232,814 PS points, yielding the density of 67 points/km^2 detected as a stable point in the descending area as shown in Figure 18. This area appeared to be subsidence slowly at an average rate of approximately 1.75 mm/yr. Fast relative velocity subsidence between 8 to 25 mm/yr is found in Nakorn Prathom, Samut Sakhon, and Samut Prakarn of the descending area are controlled by industrial, commercial, residential, aquaculture, and agriculture zones.

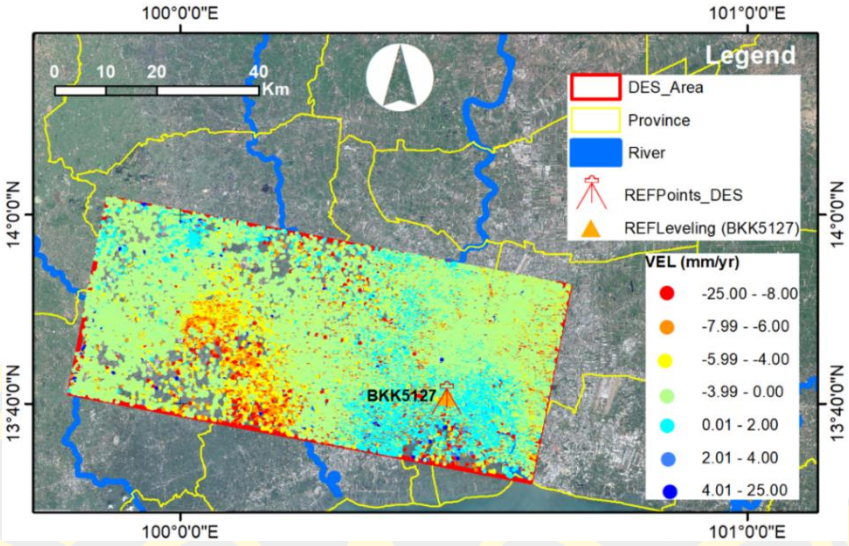

Figure 18 The relative velocity map of the PS-InSAR point from descending analyses.

Figure 17 and Figure 18, the colour circle points represent the relative velocity (mm/yr) on the line-of-sight (LOS) direction with respect to a stable area of reference leveling benchmark (BKK5217) by RTSD. The PS-InSAR reference point for two geometry orbits was selected in a relatively stable point and close to each other within 500 meters, as shown in Figure 19. The positive values are a movement toward the sensor. However, the negative values are a movement away from the sensor in Figure 16. 80 acquisitions between Jan 2016 and Sep 2019 were used in the ascending analysis, while 93 acquisitions between Jan 2016 and Oct 2019 were used in the descending analysis.

The BKK5217 reference point of this research is located at the Khlong Bang Khun Thian Bride, Rama II road, Chom Thong District, Bangkok Thailand, That the depth of benchmark through the sand bed is subsurface on the Earth. In Figure 19 as the selection of PS-InSAR points should have temporal coherence more than 0.8 or higher. So, the temporal coherence of the ascending PS-InSAR reference point and descending PS-InSAR reference point has 0.95 and 0.94 due to distance among BKK5217-ascending point, BKK5217-descending point, and ascending point-descending point is 358, 337, and 462 meter in order.

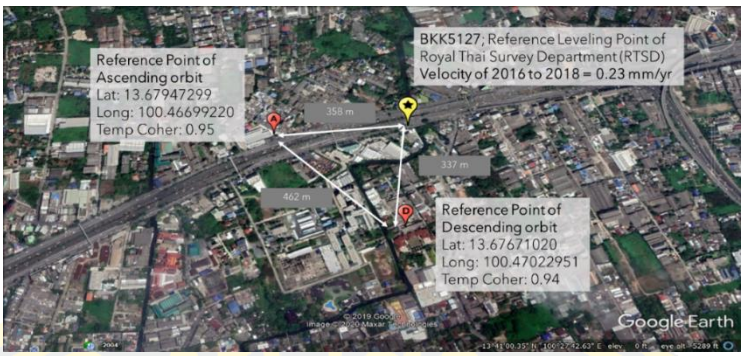

Figure 19 The location of reference leveling benchmark (star-BKK5217), Ascending PS-InSAR reference point (A) and Descending PS-InSAR reference point (D).

4.2 Validation with Benchmark Leveling

This validation analysis revealed four benchmarks (BM51, BM52, BM53, and BKK6062) in the land subsidence area of interest with the result from InSAR (Figure 20). The result was analyzed using the 95-confidence interval with land subsidence rate from leveling benchmark of RTSD and the linear regression trendline with the relative movement point of descending Sentinel-1 orbit from PS-InSAR time-series.

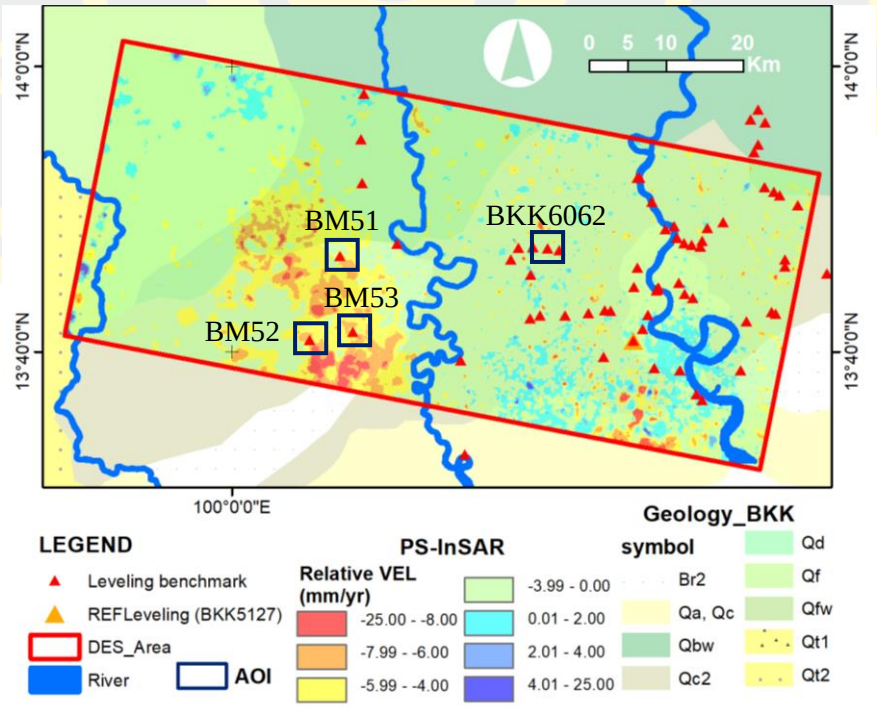

Figure 20 The four areas are shown as navy blue squares in descending Sentinel-1 area, validate between leveling benchmark of RTSD and velocity point of PS-InSAR time-series.

The BM51 leveling benchmark is located at Wat Bo Takua Phuttharam in Nakhon Chai Si district that closed to the Mueang Nakhon Pathom District, Nakhon Pathom province. The subsidence rate of leveling is 3.32 mm/year, while 4.28 mm/year is the PS-InSAR time-series subsidence rate. The linear regression (Figure 21) shown the 0.82 of subsidence rate RSQ by leveling survey form 2016 till 2018 and the time-series standard deviations (1.52 mm) of PS-InSAR points. The validation analysis as a relative movement trend of the BM51 leveling benchmark is satisfiable with the trend of relative LOS movement of PSI145484 point of descending Sentinel-1 orbit because both trendlines conform to the ninety-five-confidence interval, but the subsidence rate is a little bit higher compared to the 95 confidence interval trendline. Moreover, the urban expansion and aquaculture surrounding the BM51 is a risk zone area of land subsidence.

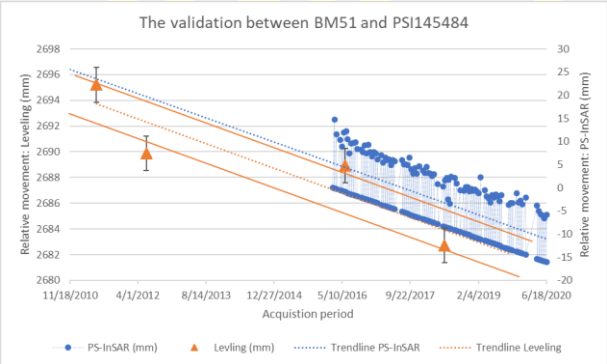

Figure 21 The validation graph of relative movement between the BM51 leveling benchmark of RTSD and the PSI145484 velocity point of PS-InSAR time-series.

The BM52 leveling benchmark is located at Watjindaram school in Sam Phran district that closed to the Ban Phaeo district, Nakhon Pathom province. The subsidence rate of leveling is 7.08 mm/year, while 6.49 mm/year is the PS-InSAR time-series subsidence rate. The linear regression (Figure 22) shown the 0.94 of subsidence rate RSQ by leveling survey form 2016 till 2018 and the time-series standard deviations (1.62 mm) of PS-InSAR points. The validation analysis as a relative movement trend of the BM52 leveling benchmark agrees with the trend of relative LOS movement of PSI215903 point of descending Sentinel-1 orbit because

both trendlines conform to the ninety-five-confidence interval. Moreover, the agriculture surrounding the BM52 is a very risk zone area of land subsidence.

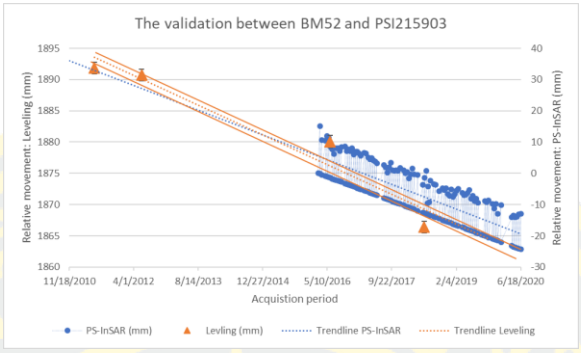

Figure 22 The validation graph of relative movement between the BM52 leveling benchmark of RTSD and the PSI215903 velocity point of PS-InSAR time-series.

The BM53 leveling benchmark is located at Wat Pridaram in Sam Phran district that closed to the Krathum Baen district, Nakhon Pathom province. The subsidence rate of leveling is 2.62 mm/year, while 3.93 mm/year is the PS-InSAR time-series subsidence rate. The linear regression (Figure 23) shown the 0.86 of subsidence rate RSQ by leveling survey form 2016 till 2018 and the time-series standard deviations (1.69 mm) of PS-InSAR points. The validation analysis as a relative movement trend of the BM53 leveling benchmark agrees with the trend of relative LOS movement of PSI207913 point of descending Sentinel-1 orbit because both trendlines conform to the ninety-five-confidence interval. Moreover, the urban expansion and agriculture surrounding the BM53 is a risk zone area of land subsidence.

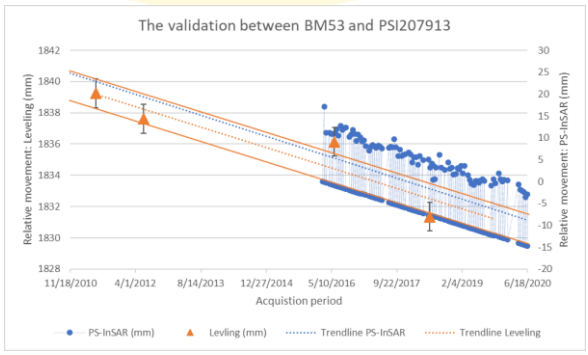

Figure 23 The validation graph of relative movement between the BM53 leveling benchmark of RTSD and the PSI207913 velocity point of PS-InSAR time-series.

The BKK6062 leveling benchmark is located at Klong Khun Si Bridge in Thawi Watthana, Bangkok. The subsidence rate of leveling is 1.84 mm/year, while 0.88 mm/year is the PS-InSAR time-series subsidence rate. The linear regression (Figure 24) shown the 0.1 of subsidence rate RSQ by leveling survey form 2016 till 2018 and the time-series standard deviations (1.41 mm) of PS-InSAR points. The validation analysis as a relative movement trend of the BKK6062 leveling benchmark is satisfiable with the trend of relative LOS movement of PSI95832 point of descending Sentinel-1 orbit because both trendlines conform to the ninety-five-confidence interval, but the 95 confidence interval trendline is rather wide owing to dispersion of leveling survey point. Moreover, the urban area surrounding the BKK6062 is rather small subsidence.

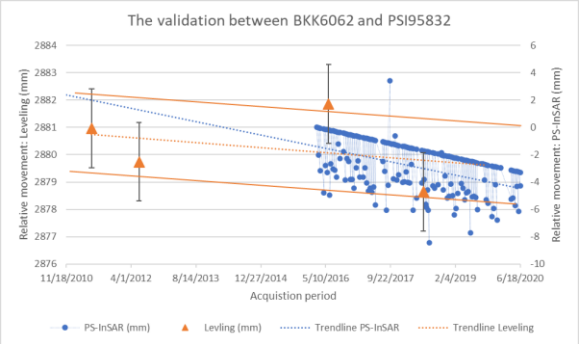

Figure 24 The validation graph of relative movement between the BKK6062 leveling benchmark of RTSD and the PSI95832 velocity point of PS-InSAR time-series.

According to Figure 21, Figure 22, Figure 23, and Figure 24, as the vertical axis represents a relative movement (mm) of leveling in the left side of the graph and relative movement of PS-InSAR (right side on y-axis or vertical axis) while the horizontal axis represents the acquisition period. The four areas of validation analysis as relative movement trendline of leveling benchmark agree with the blue dotted trendline of relative LOS movement time-series point of descending Sentinel-1 orbit from PS-InSAR because both solid orange trendlines agree with a ninety-five confidence interval. Meanwhile, the BKK6062 leveling benchmark shown a low R-squared (0.1), seen in Table 4, but the ninety-five-confidence interval and trendline of PS-InSAR are satisfied agreement.

Table 4 The statistic value of four validation pairs between PS-InSAR descending techniques and leveling benchmark techniques.

Point in AOI	Technique	Distance (m) (Figure 25)	RSQ (4 years of Leveling)	Time-series σ (mm)	2016-2019 Relative Velocity (mm/yr)
PSI145484	PS-InSAR	15.32		1.52	-4.28
BM51	Leveling		0.82		-3.32
PSI215903	PS-InSAR	196.59		1.62	-6.49
BM52	Leveling		0.94		-7.08
PSI207913	PS-InSAR	120.34		1.69	-3.93
BM53	Leveling		0.86		-2.62
PSI95832	PS-InSAR	34.89		1.41	-0.88
BKK6062	Leveling		0.1		-1.84

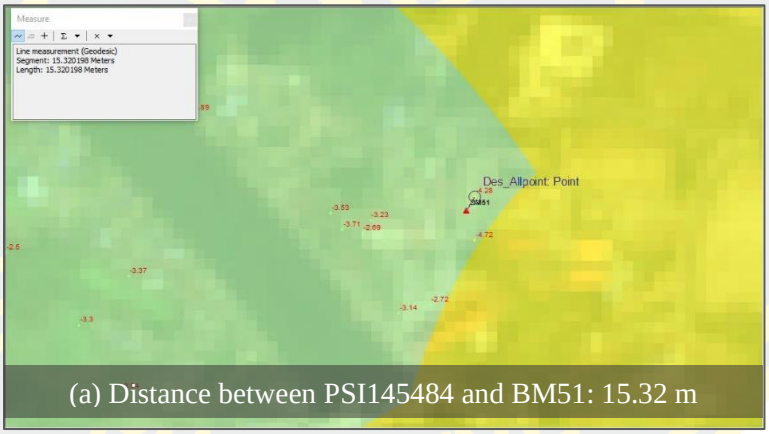

(a) Distance between PSI145484 and BM51: 15.32 m

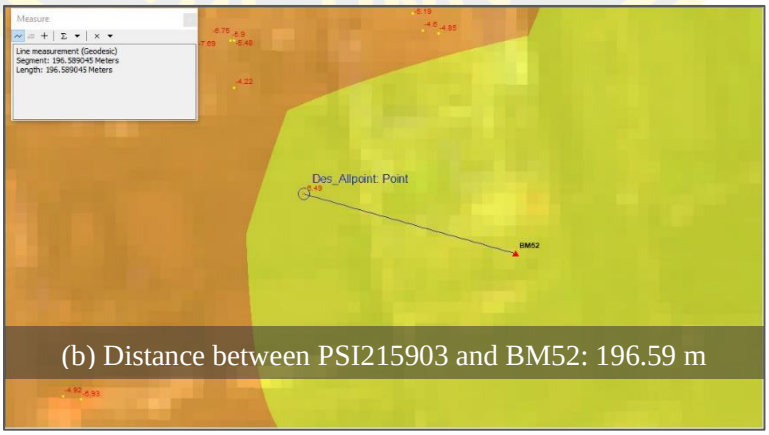

(b) Distance between PSI215903 and BM52: 196.59 m

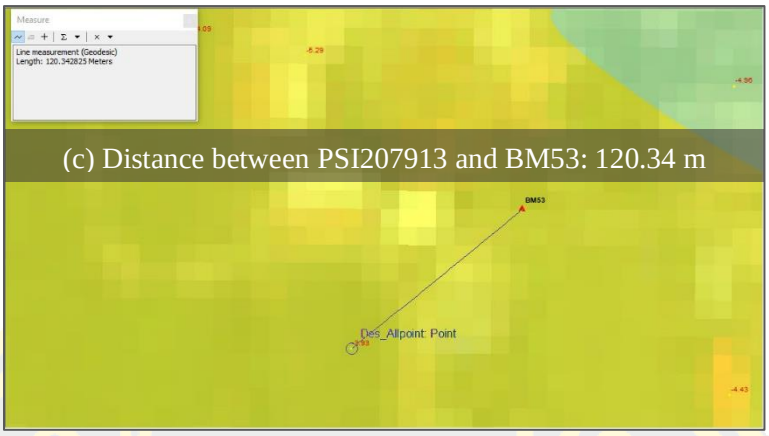

(c) Distance between PSI207913 and BM53: 120.34 m

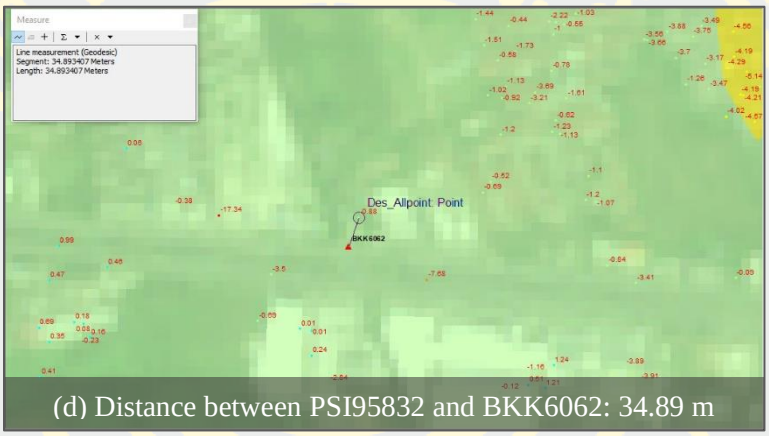

(d) Distance between PSI95832 and BKK6062: 34.89 m

Figure 25 (a-d) The nearest distance between PS-InSAR point and leveling point in AOI.

The four PS-InSAR time-series point in the Figure 21, Figure 22, Figure 23, and Figure 24 are used raw data result by SARPROZ software that the blue dotted line represents the linear regression trendline of PS-InSAR time-series points for validation with the leveling benchmark points. By the way, the linear velocity that is estimated by the SARPROZ software on the Figure 26, Figure 27, Figure 28, and Figure 29. The resulting graph by SARPROZ software also estimates a variation of deformation around the estimated overall velocity, which is based on the processing and is under the assumption that these residuals are caused by non-linear motion elements.

The four quality validation pair between PS-InSAR point and leveling point from the descending analysis were analyzed by calculating the time-series standard deviations of the linear regression line in January 2016 to October 2019. The RSQ of

trendline leveling shown high value like high accuracy from four points of leveling benchmark survey in 2011, 2012, 2016, and 2018. The standard deviations were found in the range between 1.41 mm and 1.69 mm of the descending time-series that the significantly standard deviations are lower of PS-InSAR time-series points analysis as respect to the BKK5127. However, the relative velocity of land surface movement from PS-InSAR techniques and leveling survey techniques has calculated the slope of linear regression by respecting the BKK5127 reference leveling point in a long period from 2016 till 2019. According to Table 4, the difference of validation pairs in surface displacement rates between the leveling point and PS-InSAR time-series point is in a range between 0.59 mm/year and 1.31 mm/year.

The relative descending velocity of the PS-InSAR time-series technique agrees with the leveling method by RTSD. Nevertheless, both area of ascending and descending orbits can estimate relative velocity that it may be different value as shown in Table 4. The nearest 19 points among leveling benchmark, ascending orbit, and descending orbit from 81 leveling benchmark observation in the study area. Because the Earth's surface movement is composed of horizontal and vertical movement and geometric orbit of the satellite is a difference, as seen in Figure 16. So, this research concerns the vertical subsidence in Bangkok by combined and decomposed the vertical velocity from both orbits in Bangkok's recent vertical subsidence formation on the discussion part.

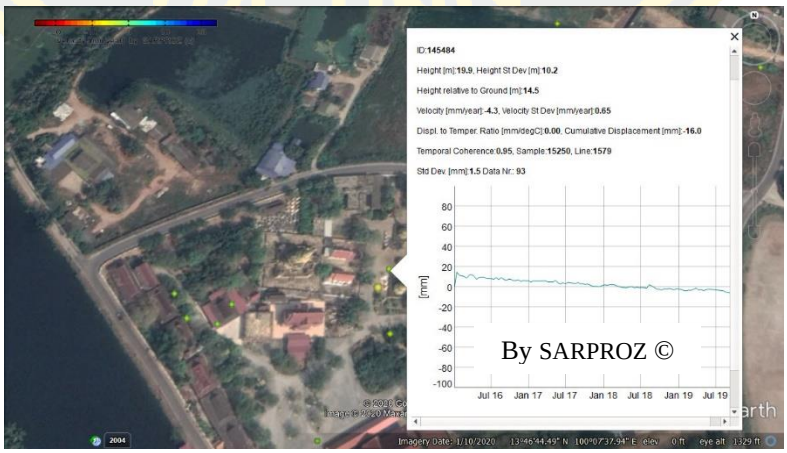

Figure 26 The result of PSI145484 by SARPROZ software on the Google Earth background.

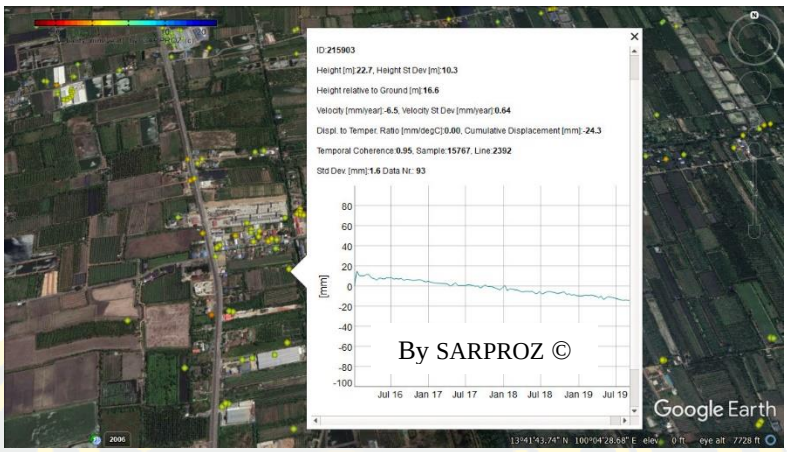

Figure 27 The result of PSI215903 by SARPROZ software on the Google Earth background.

Figure 28 The result of PSI207913 by SARPROZ software on the Google Earth background.

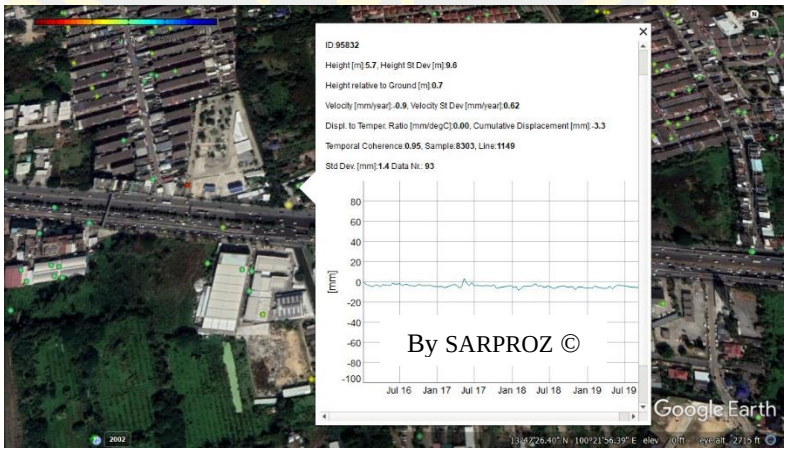

Figure 29 The result of PSI95832 by SARPROZ software on the Google Earth background.

Table 5 The relative velocity between RSQ of 0.8 or higher and significant statistics of ascending or descending orbits in the study area.

No.	Points in the study area	RSQ (4 years of Leveling)	Time-series σ (mm)	2016-2019 Relative velocity (mm/year)
1	BM51	0.82		-3.32
	DES-PSI145484		1.52	-4.28
2	BM52	0.94		-7.08
	DES-PSI215903		1.62	-6.49
3	BM53	0.86		-2.62
	DES-PSI207913		1.69	-3.93
4	BM32	0.96		0.62
	ASC-PSI3360		2.28	6.76
5	BKK640	0.96		2.29
	ASC-PSI107324		1.77	6.32
	DES-PSI153964		1.54	0
6	BKK639	0.96		1.89
	ASC-PSI103861		1.82	7.09
	DES-PSI154490		2.13	0.19
7	BM50(52)	0.80		-4.26
	DES-PSI122386		1.66	-3.98
8	BM43(50)	0.90		1.57
	DES-PSI4662		1.91	1.01
9	BKK320	0.98		-2.67
	ASC-PSI244136		2.96	-0.02
10	BKK106	0.83		5.13
	ASC-PSI119258		2.98	7.74
	DES-PSI116787		2.22	-0.76
11	BKK622-59	0.96		4.84
	ASC-PSI128492		1.97	4.65
	DES-PSI119451		1.54	-1.11
12	BKK636	0.88		3.19
	ASC-PSI101676		2.04	5.67
	DES-PSI147624		1.27	1.30

No.	Points in the study area	RSQ (4 years of Leveling)	Time-series σ (mm)	2016-2019 Relative velocity (mm/year)
13	BKK242	0.88		0.04
	ASC-PSI202181		2.2	3.73
	DES-PSI22164		1.58	-1.67
14	BKK455	0.87		-0.90
	ASC-PSI50441		1.66	-1.12
15	BKK454	0.80		-1.44
	ASC-PSI51355		2.21	-1.81
16	BM20	0.96		0.94
	ASC-PSI54895		2.19	6.17
17	BKK176-57	0.93		-3.24
	ASC-PSI22093		2.07	5.64
	DES-PSI180943		2.23	-1.79
18	BKK514	0.96		2.48
	ASC-PSI73346		1.64	8.42
	DES-PSI159135		1.70	0.94
19	BKK547	0.87		-0.98
	ASC-PSI53709		2.01	-1.78
	DES-PSI192446		1.69	0.29
REFPOINT	BKK5127	0.95		

5 DISCUSSION

5.1 The validation result

The quality result of the validation shown a satisfying agreement. So, the relative velocity of ascending and descending orbits in range direction can decompose the vertical velocity because the relative velocity of each orbit is display trend the same way result. Additionally, the four points of PS-InSAR time-series techniques were subsided, as well as a conform to 95 confidence interval trendline, also were confirmed in validation by leveling benchmark techniques. In order that the accuracy of PS-InSAR time-series techniques in Bangkok and its vicinity, is millimeter-level of land subsidence by linear in time. Because this technique considers the C-band Sentinel-1 sensor, a large quantity of SAR images (80 and 93 images), a long-time period (2016-2019), acceptable distance from the reference point, and high coherence of the PS as seen in Figure 33 for pleasant accuracy. As a result, the PS-InSAR time-series can evaluate the precise vertical velocity of land subsidence due to the validation between leveling and PS-InSAR method.

5.2 Evaluation of the Performance of Sentinel-1 PS-InSAR Time-series Technique

Measuring the vertical movement of land subsidence of such a wide ground area is hence difficult and using high cost or many people from geodetic tools such as GNSS, leveling while the InSAR techniques can also obtain the high accuracy movement when the Earth's surface movement, as seen in Table 3. The Sentinel-1 PS-InSAR time-series analysis is a good performance because a large number of sentinel-1 datasets in both ascending and descending geometries have a short revisit time on C-band like the up-to-date high spatial resolution data. That all benefits with the spatial-temporal baseline offer the significant potential and accuracy of measuring land subsidence in this research.

The hexagonal area of interest has been generated with 56 grid points in 25 km^2 and found the average LOS velocity for each grid point, after that composed vertical velocity by Equation 3 and Equation 4. A standard division of the kriging method has interpolated the 56 vertical velocity points (Figure 30 as show pale green

dot). As shown in Table 6, the number of grid-point on this table is ordered left-bottom (Grid-Point No.1) to right-top (Grid-Point No.56), as seen in Figure 30 also. While the 51 leveling benchmark (Figure 31 as show red triangle and Table 7 as explain the detail such as elevation on each year, leveling station, and type of leveling benchmark) is less attribution. Even the spatial resolution, spatial characteristics, temporal aspects, human resources, observation density, and accuracy factors are the difference between PS-InSAR techniques and leveling surveys. However, the two technique methods can support and eliminate of a different problem.

Table 6 The vertical velocity (mm/year) by combined PS-InSAR time-series analysis from different orbits.

Grid-Point No.	Density of ASC (points)	% Density of ASC	Density of DES (points)	% Density of DES	Vertical Velocity (mm/yr)	Grid-Point No.	Density of ASC (points)	% Density of ASC	Density of DES (points)	% Density of DES	Vertical Velocity (mm/yr)
1	1438	0.72	1682	0.93	-18.79	**29**	5296	2.66	4248	2.35	-6.79
2	2397	1.20	1980	1.10	-20.01	**30**	614	0.31	821	0.45	-8.64
3	1315	0.66	1152	0.64	-14.31	**31**	922	0.46	1418	0.79	-6.36
4	565	0.28	454	0.25	-7.16	**32**	2171	1.09	2293	1.27	-6.89
5	2101	1.06	1270	0.70	-9.43	**33**	2793	1.40	2250	1.25	-6.08
6	1793	0.90	2542	1.41	-14.56	**34**	3733	1.87	3473	1.92	-7.38
7	2019	1.01	2667	1.48	-16.34	**35**	3978	2.00	4189	2.32	-7.95
8	2045	1.03	2722	1.51	-16.37	**36**	5979	3.00	5710	3.16	-10.56
9	3766	1.89	3076	1.70	-11.75	**37**	7255	3.64	6609	3.66	-6.60
10	2969	1.49	2534	1.40	-9.86	**38**	7207	3.62	5418	3.00	-4.41
11	5351	2.69	4200	2.33	-14.19	**39**	3355	1.68	1996	1.11	-3.60
12	3346	1.68	2916	1.61	-13.49	**40**	267	0.13	541	0.30	-8.28
13	3904	1.96	4845	2.68	-8.40	**41**	458	0.23	783	0.43	-5.81
14	3121	1.57	3850	2.13	-13.21	**42**	610	0.31	672	0.37	-4.42
15	4302	2.16	4819	2.67	-11.99	**43**	759	0.38	839	0.46	-5.94
16	5014	2.52	4325	2.40	-11.08	**44**	3365	1.69	3110	1.72	-9.75
17	5806	2.92	3630	2.01	-9.07	**45**	3248	1.63	3581	1.98	-8.31
18	5834	2.93	4213	2.33	-12.30	**46**	6110	3.07	5221	2.89	-6.02
19	5200	2.61	5311	2.94	-15.28	**47**	6885	3.46	4952	2.74	-3.60
20	2597	1.30	2255	1.25	-12.93	**48**	6285	3.16	4892	2.71	-3.71
21	6830	3.43	3696	2.05	-6.73	**49**	4526	2.27	3443	1.91	-0.20
22	1740	0.87	1915	1.06	-10.08	**50**	254	0.13	225	0.12	-6.53
23	2849	1.43	2715	1.50	-7.29	**51**	152	0.08	236	0.13	-2.04
24	3095	1.55	2851	1.58	-8.82	**52**	1750	0.88	1889	1.05	-4.01
25	3787	1.90	3431	1.90	-7.08	**53**	4694	2.36	5312	2.94	-6.57
26	7908	3.97	5391	2.99	-12.56	**54**	3672	1.84	3722	2.06	-7.12
27	8348	4.19	8165	4.52	-13.71	**55**	4686	2.35	4956	2.74	-5.00
28	5854	2.94	5948	3.29	-9.00	**56**	2808	1.41	3218	1.78	-1.74

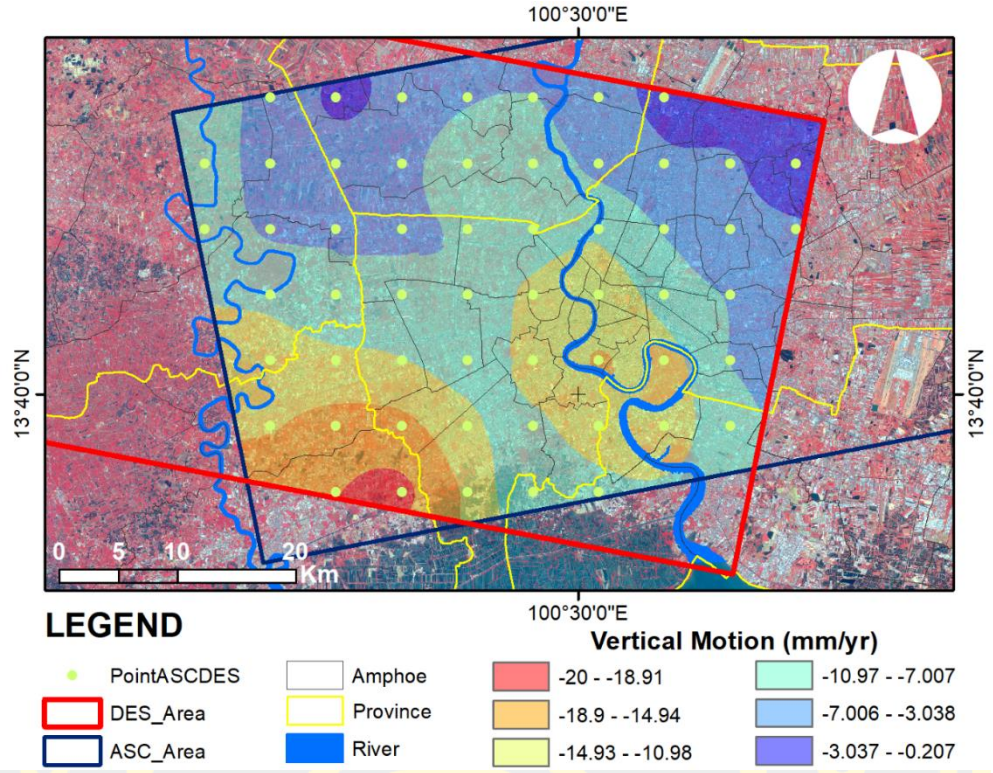

Figure 30 The vertical velocity decomposes by the velocity of ascending and descending geometries.

The hexagon interesting area vertical motion between 2016 to 2019 in Figure 30 presents the subsidence rate from 0.2 to 20 mm/year occurred in the Western Greater Bangkok (Bangkok, Samut Sakhon, Samut Prakan, Nonthaburi, and Nakhon Pathom provinces). The land subsidence situation presents a high subsidence movement (15-20 mm/year) in Muang Samut Sakhon and Bang Khlo subdistrict, Bang Kho Laem district, and Chong Nonsi subdistrict, Yan Nava district close to Chao Phraya River in Bangkok. While Lak Si, Bang Ken, Bung Kum, Khan Na Yao districts in Bangkok, and Nong Phrao Ngai village, Sai Noi Districts in Nonthaburi province was the subsidence rate between 0.2 to 3 mm/year. The high subsidence movement on the red zone (Figure 30) seems to happen in the industrial, commercial, aquaculture, agriculture, and residential zone of Muang Samut Sakhon in Samut Sakhon province. The orange zone in the central of Bangkok represents the quite high subsidence rate because this area is medium - high density residential zone and commercial zone according to The Bangkok Comprehensive Plan 2013 (B.E.2556) by the Department of City Planning, BMA.

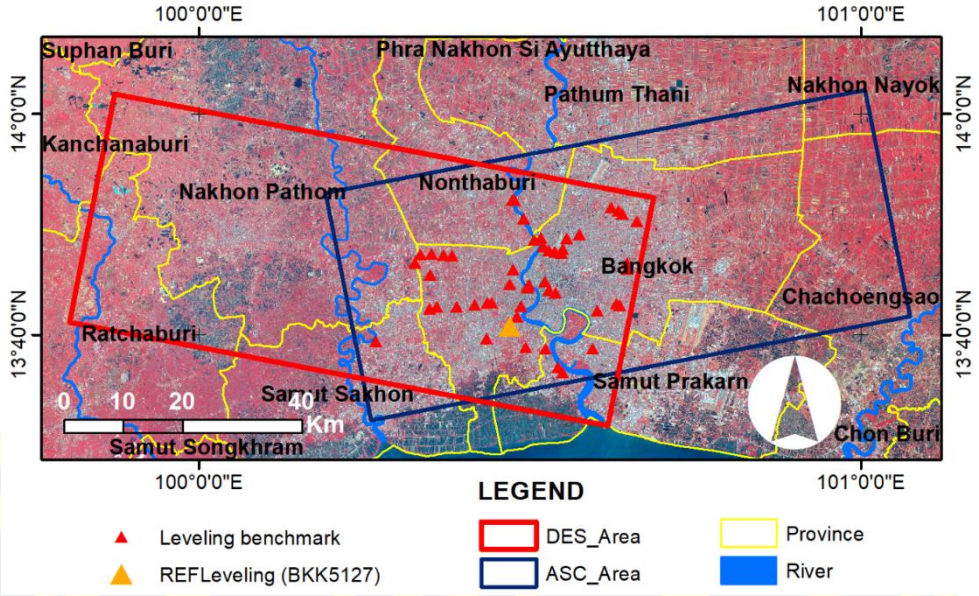

Figure 31 The 51 leveling benchmarks in the hexagon area between ascending and descending orbits.

Table 7 Detail of 51 leveling benchmark surveying by DRTS in the hexagon area between ascending and descending orbits.

Leveling No.	Station	Leveling Type	Elevation (mm) by DRTS				Velocity (mm/year)		
			2011	2012	2016	2018	Four points on 2011-2018	Two points on 2016-2018	Relative of two points on 2016-2019
1	BM39	BM	1481.87	1472.08	1483.61	1478.50	0.38	-2.56	-2.78
2	BKK663	drill	2169.86	2163.19	2176.48	2179.60	1.93	1.56	1.34
3	BM19	BM	1647.22	1649.91	1658.89	1663.47	2.30	2.29	2.07
4	BKK640	hold	2039.32	2043.95	2048.97	2054.00	1.88	2.52	2.29
5	BKK639	drill	2844.42	2848.89	2853.89	2858.12	1.77	2.12	1.89
6	BKK37629-47	drill	2420.65	2416.10	2420.77	2422.56	0.54	0.90	0.67
7	BKK6061	drill	3497.47	3497.31	3502.85	3500.39	0.63	-1.23	-1.46
8	BKK6062	drill	2880.96	2879.74	2881.86	2878.64	-0.13	-1.61	-1.84
9	BKK6063	drill	3043.24	3039.80	3042.10	3041.08	-0.07	-0.51	-0.74
10	BKK6064	drill	3716.35	3711.17	3713.84	3711.17	-0.37	-1.34	-1.56
11	BM37	BM	1900.94	1889.45	1894.55	1898.89	0.21	2.17	1.95
12	BKK2079	hold	1592.52	1590.64	1580.67	1592.20	-0.54	5.77	5.54
13	BKK277	drill	1475.00	1473.85	1466.13	1480.86	0.28	7.37	7.14
14	BKK206	drill	4451.03	4448.55	4420.86	4429.15	-3.95	4.15	3.92
15	BKK209	hold	3148.99	3147.85	3144.23	3161.99	1.31	8.88	8.66

Leveling No.	Station	Leveling Type	Elevation (mm) by DRTS				Velocity (mm/year)		
			2011	2012	2016	2018	Four points on 2011-2018	Two points on 2016-2018	Relative of two points on 2016-2019
16	BKK210	drill	2223.02	2221.15	2213.03	2228.49	0.22	7.73	7.51
17	BKK222	hold	1459.04	1453.95	1446.76	1462.19	0.05	7.72	7.49
18	BKK215	drill	2275.47	2271.39	2262.09	2269.76	-1.09	3.84	3.61
19	BKK216	drill	1567.83	1565.39	1556.33	1570.32	-0.16	7.00	6.77
20	BKK284	hold	2349.83	2346.68	2350.78	2347.86	0.04	-1.46	-1.69
21	BM33	BM	1986.29	1985.56	1990.52	2010.13	3.01	9.81	9.58
22	BKK682	hold	2387.41	2387.05	2391.04	2389.28	0.43	-0.88	-1.11
23	BM18	BM	882.15	874.96	879.95	893.04	1.62	6.55	6.32
24	BKK236-31	drill	897.07	888.71	895.15	907.68	1.69	6.27	6.04
25	BKK159	drill	1827.48	1816.97	1816.44	1825.57	-0.09	4.57	4.34
26	BKK160	drill	566.88	561.61	560.83	570.47	0.45	4.82	4.60
27	BKK162	drill	986.12	984.05	977.78	988.70	-0.01	5.46	5.24
28	BKK124	drill	1031.33	1030.50	1028.35	1045.08	1.47	8.37	8.14
29	BM8	BM	1647.78	1646.61	1639.94	1653.33	0.30	6.70	6.47
30	BKK115	drill	1297.29	1299.84	1298.11	1310.62	1.39	6.26	6.03
31	BM7	BM	1668.97	1670.76	1669.83	1679.42	1.12	4.80	4.57
32	BKK106	hold	2067.97	2072.16	2074.37	2085.09	2.01	5.36	5.14
33	BKK502	hold	2504.99	2507.63	2507.86	2519.27	1.61	5.71	5.48
34	BM1	BM	2229.06	2226.42	2216.53	2228.45	-0.56	5.96	5.74
35	BKK612	drill	4520.29	4521.38	4509.13	4521.46	-0.54	6.17	5.94
36	BKK622-59	drill	3600.57	3598.86	3674.57	3684.71	13.71	5.07	4.85
37	BKK636	drill	2205.49	2207.25	2209.94	2216.78	1.41	3.42	3.20
38	BKK637	drill	1727.49	1729.98	1732.55	1738.72	1.39	3.09	2.86
39	BKK241	hold	2394.78	2392.73	2390.70	2395.52	0.01	2.41	2.19
40	BKK242	hold	1485.13	1484.85	1480.98	1481.51	-0.62	0.27	0.04
41	BM16	BM	1707.74	1705.42	1705.28	1709.33	0.21	2.03	1.80
42	BKK255	hold	2256.13	2255.41	2251.48	2257.37	-0.06	2.95	2.72
43	BKK176-57	hold	2162.80	2156.00	1002.47	996.44	-195.09	-3.02	-3.24
44	BKK5110	drill	1709.23	1721.86	1735.44	1728.23	2.71	-3.61	-3.83
45	BKK5111	drill	1948.51	1956.54	1970.08	1963.45	2.31	-3.32	-3.54
46	BKK5112	drill	2068.61	2074.01	2087.44	2082.03	2.17	-2.71	-2.93
47	BM11	BM	1754.71	1756.92	1754.35	1761.04	0.55	3.35	3.12
48	BKK514	hold	1421.57	1425.55	1430.41	1435.83	1.83	2.71	2.49
49	BKK5127	drill	3345.95	3349.38	3359.73	3360.18	2.13	0.23	0.00
50	BKK533	drill	1109.32	1118.57	1134.81	1121.39	2.11	-6.71	-6.94
51	BKK547	drill	990.92	995.76	1006.22	1004.72	2.07	-0.75	-0.98

* BM (ground surface subsidence) leveling benchmark: through sedimentary (sand) bed depth (approximately 20 m) and BKK vertical leveling benchmark: two types (drill and hold) and depth through a sand bed.

Besides, the horizontal velocity in the study area is derived by combined and decomposed the ascending and descending orbits by Equation 3, Equation 4 and interpolation by the standard division of the kriging method in the overlapping area also. Figure 32(b) almost presents the negative value of the horizontal motion rate from 2.88 to 29.13 mm/year in descending Azimuth Look Direction (ALD), as seen Figure 16(b). Nevertheless, the two points of 56-decomposing velocity are display positive horizontal movement. The first point (0.75 mm/year) is located at Lat Yao subdistrict, Chatuchak District, Bangkok and the other (0.2 mm/year) is located at Khae Rai subdistrict, Krathum Baen District, Samut Sakhon province. An average rate of subsidence and left horizontal movement of descending ALD are 8.93 mm/year and 13.86 mm/year. The spatial pattern of vertical and horizontal motion map is in the same way, as shown in Figure 32.

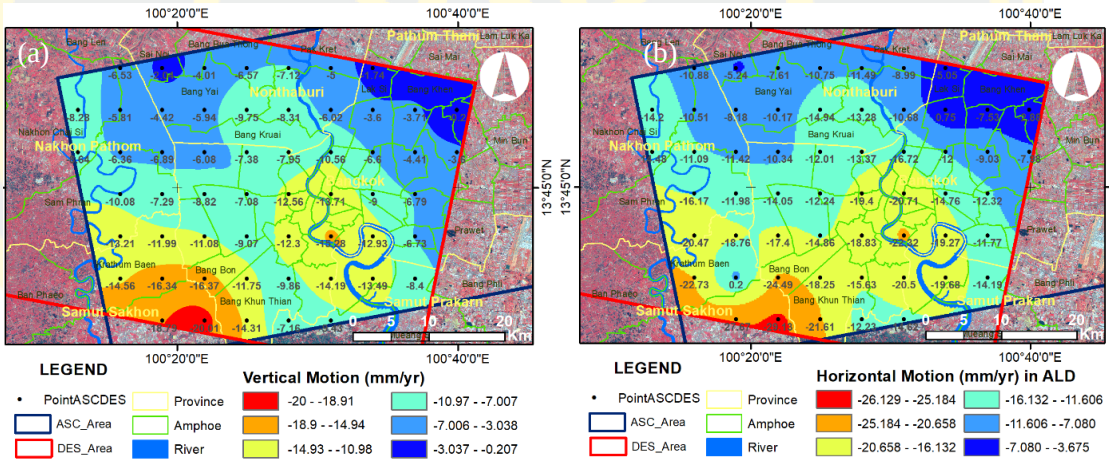

Figure 32 The vertical (a) and horizontal (b) motion maps in the hexagon interesting area between 2016 to 2019.

5.3 Limitations of the PS-InSAR Time-series Technique

Thailand located in the tropical zone of ASIA, so almost agriculture environment, as seen in Figure 17, is located in Mueang Chachoengsao, Bang Nam Priao, in Chachoengsao, Ongkharak in Nakhon Nayok, and Lan Luk Ka in Pathum Thani located on the top-right side of ascending study area. This area controlled by vegetation that has high decorrelation or low coherence (dark blue colour) as shown in Figure 33. So caused this area, shown a lower density (white background colour) of Persistent Scatterer pixels as shown in Figure 34. The PS-InSAR time-series

technique can detect high coherence area from the stable area such as urban area. Nevertheless, It is challenging to detect the extreme decorrelation either the movement or non-stationary objects such as fall off, bloom, blown away.

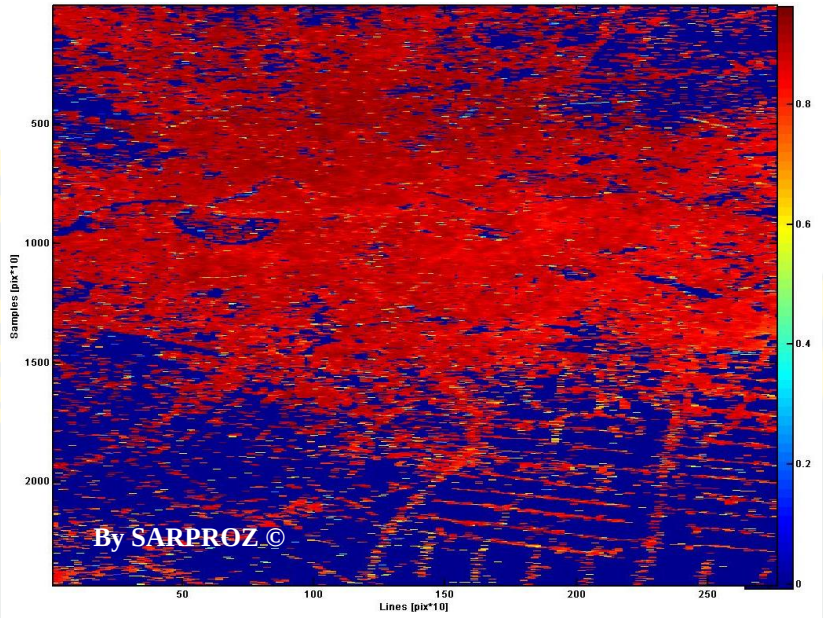

Figure 33 The coherence map in ascending orbit using PS-InSAR techniques by SARPROZ software (The dark red represents high coherence while the dark blue represents low coherence)

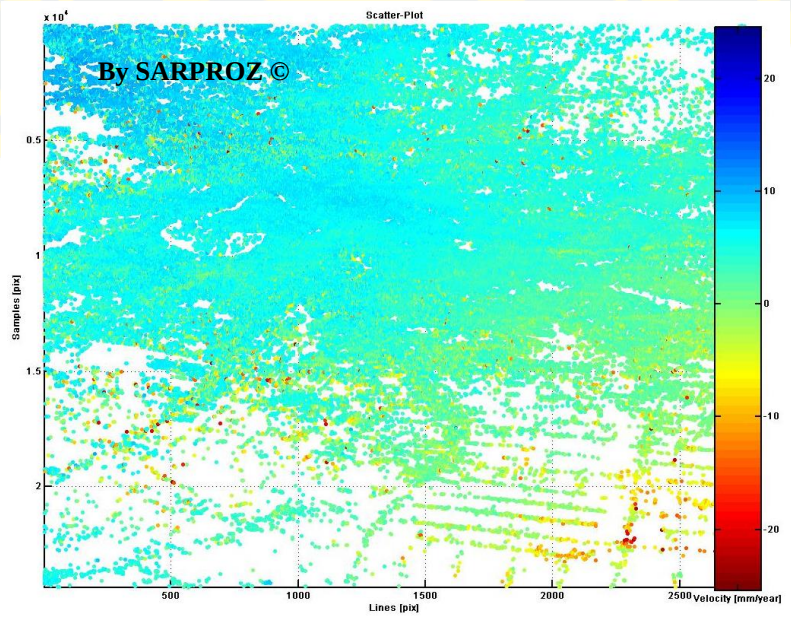

Figure 34 The Persistent Scatterer plot in ascending orbit using PS-InSAR techniques by SARPROZ software (The white background colour is no Persistent Scatter pixel)

5.4 The formation of recent vertical subsidence in Bangkok

The vertical motion map (Figure 30) in the hexagonal area of interest illustrates two separate areas of maximum subsidence. The NNW-trending elongate eastern subsidence area covers an area of 207 sq.km (including the orange and yellow colour zone) with the maximum vertical motion of the junction boundary among Yannawa, Rat Burana, and Bang Kho Laem districts in the center. The extremely vertical subside in the red zone, covering the 16 sq.km on Mueang Samut Sakhon district in the west area, is 19-20 mm/year.

Both spatial patterns of vertical velocity by PS-InSAR time-series technique are harmonized with the comprehensive plan in central Bangkok and land use in the SW of Bangkok area and Mueang Samut Sakhon district. Firstly, The 207 sq.km in the orange and yellow zone of subsidence as seen in Figure 30 occurred on medium-high density residential zone, and commercial zone according to The Bangkok Comprehensive Plan 2013 (B.E.2556) by the Department of City Planning, Bangkok Metropolitan Administrator as shown in Figure 35. Secondly, high vertical subsidence like the red zone at Khok Krabue, Ban Nam Chuet, and Phanthai Norasing in Mueang Samut Sakhon district is controlled by industrial, commercial, aquaculture, and residential zone as shown in Figure 36.

The reginal scale, both maximum subsidence areas are located in the Thon Buri Basin, as shown in Figure 4, which is a N-S to NW-trending Cenozoic basin (Searle & Morley, 2019). Therefore the vertical motion pattern may reflect a control by its underling basin structure. However, the correlation pattern between subsidence and the deep structure should be made with caution. Because the study area is relatively small and associated with various geomorphologies as shown in Figure 37. Thermal subsidence in this region has been developed in regional scale since the Late Miocene (Morley, 2015). The study is smaller than the Thon Buri Basin, but the vertical pattern by PS-InSAR time-series technique can refer the symbolically significant of subsidence the be similar to the trending of Chao Phraya structure in Thon Buri Basin. Not only are these factors correlated with land subsidence but also an over-pumping on groundwater, and the expansion of the urban area are the main

factor-induced subsidence disaster. Because both areas is a critical zone of groundwater level induced land subsidence (DGR, 2009).

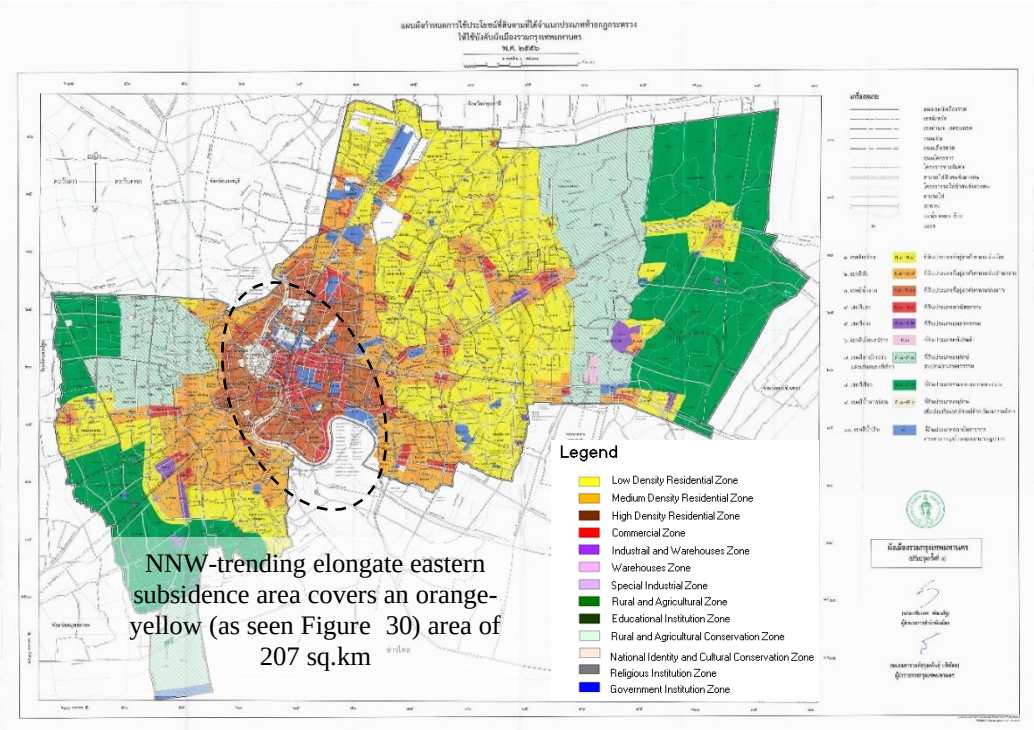

Figure 35 The land-use zoning plan of the Bangkok Comprehensive Plan 2013 (B.E.2556) by the Department of City Planning, Bangkok Metropolitan Administrator.

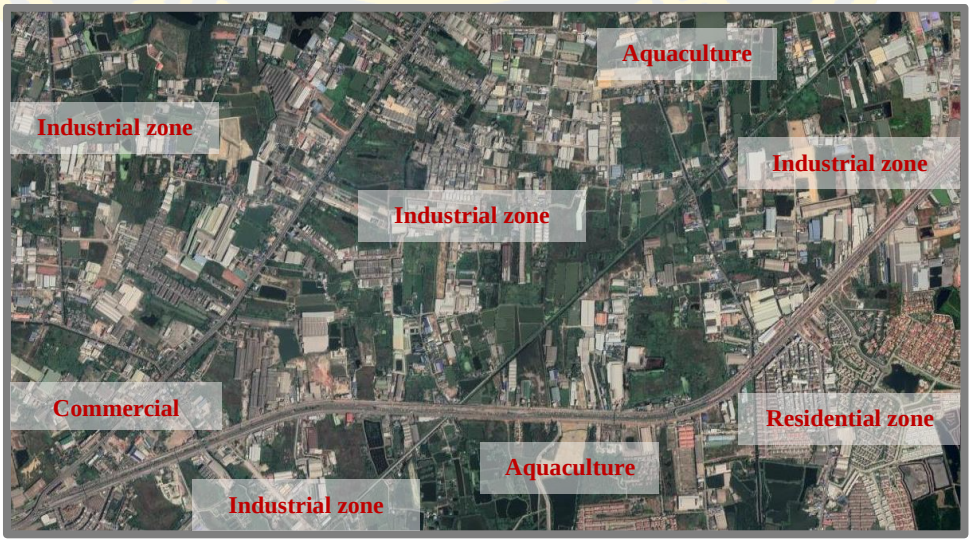

Figure 36 The extremely vertical subside in the red zone, as seen in Figure 30, covering the 16 sq.km on Mueang Samut Sakhon district.

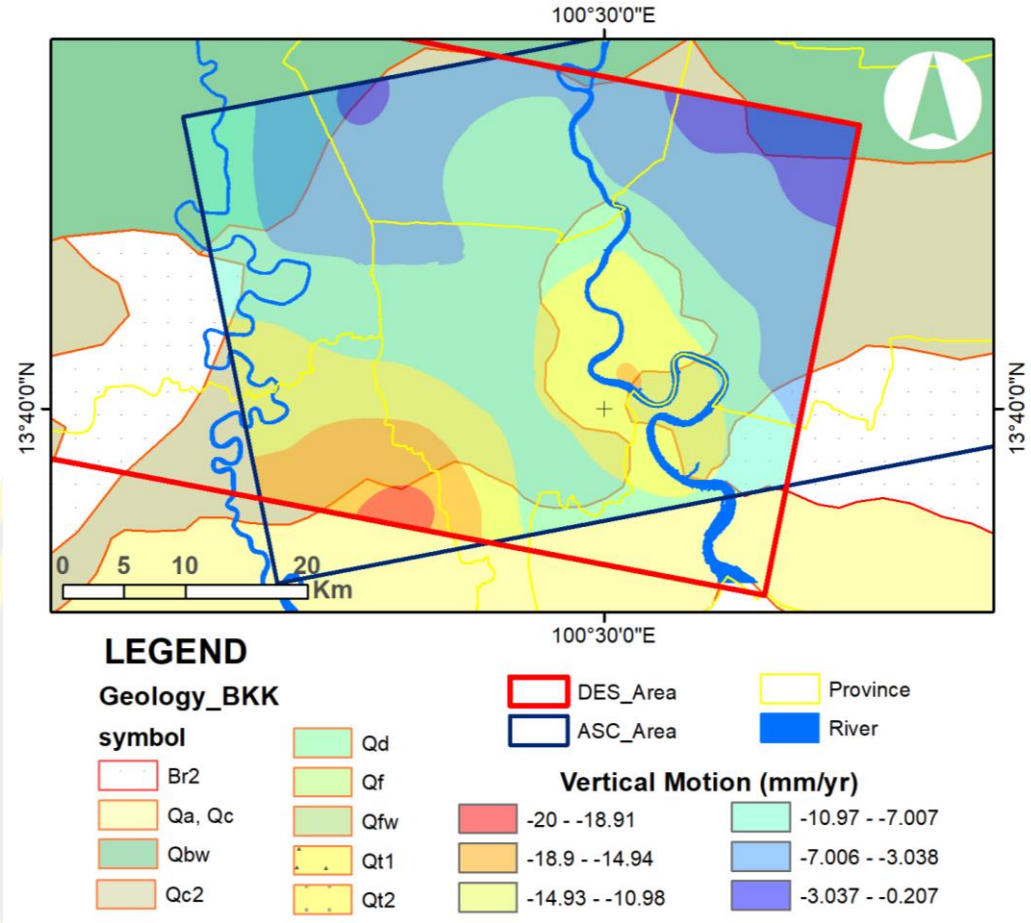

Figure 37 The vertical motion zone (mm/year) of an interesting hexagon area on the quaternary deposits map.

6 CONCLUSIONS AND RECOMMENDATIONS

6.1 Conclusions

This research used the open Sentinel-1 data acquired from ascending and descending ESA satellite data. The 80 images on 172-ascending track and the 93 images on 62-descending orbit cover the time-period from 2016 to 2019. These long-time data are appropriate for measuring land subsidence using the PS-InSAR time-series technique; the maximal annual subside rate of 25 mm/year in the LOS direction of ascending and descending orbit. The eighty points/km^2 was the density of permanent/persistent scatterers on the ascending orbit, as well as the descending path, consisted of 67 points/km^2. According to both orbits, the PS-InSAR time-series analysis represented the vertical movement as average subside 8.93 mm/year in the hexagonal area of interest.

The hexagonal area of extremely vertical subsidence is 20 mm/yr by combining and decomposing the relative velocity in both orbits. The Bangkok land subsidence, induced by over-exploration groundwater, soft Bangkok clay beneath the surface, and overload of building construction, with and hexagonal interesting are of approximately 1700 sq.km, is one of the geological hazards in lower central of Thailand. In the validation between the PS-InSAR and the precise leveling technique showed a satisfying agreement. So, the PS-InSAR time-series technique can apply to measure the ground deformation in the urban areas. In addition, this technique is resource-saving and cost-effective as possible such as human resources, cost, period time, and scope of working. The urban expansion in Mueang of Nakhon Prathm province, the industry and aquaculture in Samut Prakarn, and agriculture in Samut Sakhon are critical land subsidence areas.

Nowadays, spaceborne radar satellites provided SAR data as more and different Satellite data, whereby the download the radar data access on the website such as http://scihub.copernicus.eu/ and https://search.asf.alaska.edu/#/. The ESA's Sentinel-1 satellite mission provides the up-to-date (6 or 12 days of revisit time) high spatial resolution on range cross azimuth (5 m x 20 m) Synthetic Aperture Radar images over a 250 km x 250 km wide surface coverage. The PS-InSAR time-series

techniques can estimate the slow surface movement in a long period, but this technique also attends the decorrelation or source error.

6.2 Recommendations

The PS-InSAR time-series technique help in measuring the Earth's surface deformation, understanding of dynamic's Earth, and overcome limited the decorrelation of temporal and geometrical. Besides, the number of points provided by PS-InSAR and its density has largely overcome the under-sampling and bias problem of leveling data. In some vegetated areas had low the density of points. In future research, the analysis of the main subsiding area is suggested that land subsidence in Bangkok was mainly caused by the over-extraction of groundwater, with its spatial pattern being also controlled by geological structure subsidence in a large area or reginal basin. The quaternary basin in the central plain of Thailand is one of the important places in Thailand; it needs monitoring of subsidence because it is the most populated metropolitan area and the economic and political heart of Thailand. In this case, PS-InSAR can be used to measure the land subsidence and find factor of subsidence that influence or induce at Bangkok subsidence, and this shows the potential and limitation of radar interferometry approaches and their applicability for structural and ground deformation monitoring, including the advantages and challenges of these approaches in the study area.

The results and analysis of measuring land subsidence with PS-InSAR in Bangkok using Sentinel-1 time-series techniques shown high accuracy in millimeter-level of the subsidence rate in line-of-sight direction and the vertical movement whereby combined and decomposed both orbits of SAR images. However, the science technology for measuring the land subsidence among ground surface, space-based InSAR, the space-based geodetic method is precious to solve the geological hazard or disaster phenomena. So, future work and improvement are to integrate the PS-InSAR data worked together with groundwater level change, geomorphology, stratigraphic, structure geology, land use-landcover/green level change, sea-level rise, and associated with GIS-aided analysis for generating the land subsidence susceptibility model.

REFERENCES

(JICA), J. I. C. A. (1995). *The study on management of groundwater and land subsidence in the Bangkok Metropolitan Area and its vicinity. Report submitted to the Department of Mineral Resources. Bangkok: JICA*. Retrieved from Bangkok:

Aobpaet, A. (2012). *InSAR time series analysis for land subsidence monitoring in Bangkok and its vicinity area.* (Doctoral dissertation), Chulalongkorn University, Bangkok.

Balz, T. (2019). *Surface Motion Estimation: Lecture Note for Summer School 2019*. LIESMARS, Wuhan University, China.

Benattou, M. M., Balz, T., & Liao, M. (2018). Measuring surface subsidence in Wuhan, China with Sentinel-1 data using PSInSAR. *nternational Archives of the Photogrammetry, Remote Sensing and Spatial Information Sciences - ISPRS Archives, 42*(3), 73-77. doi:10.5194/isprs-archives-XLII-3-73-2018

Berardino, P., G. Fornaro, R. Lanari, E. Sansosti. (2002). A New Algorithm for Surface Deformation Monitoring Based on Small Baseline Differential SAR Interferograms. *IEEE Transactions on Geoscience and Remote Sensing, 40*(11), 2375-2383.

Brand, E. W., & Balasubramaniam, A. S. (1976). Soil Compressibility and Land Subsidence in Bangkok. *the International Association of Hydrological Sciences, Proceedings of the Anaheim Symposium, California, USA, 121*(December).

Chaithavee, S. (2015). *InSAR time-series analysis for land subsidence monitoring in eastern greater Bangkok.* (Master's dissertation), Chulalongkorn University, Bangkok.

Cox, J. B. (1968). *A review of engineering properties of the recent marine clay in Souttheast Asia*. Retrieved from Bangkok, Thailand:

David, G. Z. a. E., Wakshal. (2013). *Land Subsidence Analysis in Urban Area: The Bangkok Metropolitan Area Case Study*: Springer Environmental Science and Engineering.

DGR. (2009). *Study the cause of land subsidence in Bangkok and surrounding provinces*. Retrieved from Bangkok, Thailand:

DGR. (2012). *The surveying project and momitoring land subsidence system in the groundwater crisis area*. Retrieved from Bangkok, Thailand:

Eckardt, R., Urbazaev, M., Salepci, N., Pathe, C., Schmullis, C., Woodhous, I., & Stewart, C. (2019). Introduction to Radar Remote Sensing. In *ECHOES IN SPACE* (pp. 1-46): CC-BY-SA 'EO College'.

Elliott, J. R., Walters, R. J., & Wright, T. J. (2016). The role of space-based observation in understanding and responding to active tectonics and earthquakes. *Nature Communications, 7*, 1-16. doi:10.1038/ncomms13844

Ferretti, A., Prati, C., & Rocca, F. (2000). Nonlinear subsidence rate estimation using permanent scatterers in differential SAR interferometry. *IEEE Transactions on Geoscience and Remote Sensing, 38*(5 I), 2202-2212. doi:10.1109/36.868878

Ferretti, A., Prati, C., & Rocca, F. (2001). Permanent scatterers in SAR interferometry. *IEEE Transactions on Geoscience and Remote Sensing, 39*(1), 8-20. doi:10.1109/36.898661

Ferretti, A., Tamburini, A., Novali, F., Fumagalli, A., Falorni, G., & Rucci, A. (2011).

Impact of high resolution radar imagery on reservoir monitoring. *Energy Procedia*, *4*(December), 3465-3471. doi:10.1016/j.egypro.2011.02.272

Ferretti, A. P., C.; Rocca, F. (1999). *Permanent scatterers in SAR interferometry.* Paper presented at the Proceedings of the IEEE1999 International Geoscience and Remote Sensing Symposium, Piscataway, NJ, USA.

Fryksten, J., & Nilfouroushan, F. (2019). Analysis of clay-induced land subsidence in Uppsala City using Sentinel-1 SAR data and precise leveling. *Remote Sensing, 11*(23), 1-17. doi:10.3390/rs11232764

Fuhrmann, T., & Garthwaite, M. C. (2019). Resolving three-dimensional surface motion with InSAR: Constraints from multi-geometry data fusion. *Remote Sensing, 11*(3). doi:10.3390/rs11030241

GEO2TECDI-SONG. (2013). Sea level changes around Thailand; GEO2TECDI-SONG Final Symposium 27 May 2013 , Crowne Plaza , Bangkok Lumpini Park. In (Vol. May). Bangkok, Thailand: Technologies for Thailand: Environment Change Direction and Investigation-Sea Offensive Next Generation (GEO2TECDI-SONG).

Gudmundsson, S., Sigmundsson, F., & Carstensen, J. M. (2002). Three-dimensional surface motion maps estimated from combined interferometric synthetic aperture radar and GPS data. *Journal of Geophysical Research: Solid Earth, 107*(B10), ETG 13-11-ETG 13-14. doi:10.1029/2001jb000283

Gupta, R. P. (2002). *Remote Sensing Geology* (second edition ed.): Springer.

Hanssen, R. F. (2001). *Rader Interferometry: Data Interpretation and Error Analysis* (2 ed. Vol. 2): Kluwer Academic Publishers.

Hooper, A., Bekaert, D., Spaans, K., & Arikan, M. (2012). Recent advances in SAR interferometry time series analysis for measuring crustal deformation. *Tectonophysics, 514-517*, 1-13. doi:10.1016/j.tecto.2011.10.013

Hooper, A. J. (2006). *Persistent Scaterers Radar Interferometry for crustal Deformation Studies and Modeling of Volcanic Deformation.* (Doctor of Philosophy), Stanford University,

Hooper, A. J., Segall, P., & Zebker, H. (2007). Persistent scatter radar interferometry for crustal deformation studies and modeling of volcanic deformation. *Journal of Geophisical Research Solid Earth, 112*(July), 124.

Horpibulsuk, S., Yangsukkaseam, N., Chinkulkijniwat, A., & Du, Y. J. (2011). Compressibility and permeability of Bangkok clay compared with kaolinite and bentonite. *Applied Clay Science, 52*(1-2), 150-159. doi:10.1016/j.clay.2011.02.014

Inc., H. A. (1970). *Effect of Deep Well Pumping on Land Subsidence in Bangkok, part of "Master Plan, Water Supply and Distribution, Metropolitan Bangkok, Thailand". 4, Report by Camp, Dresser & Mckee Inc., submitted to Metropolitan Water Works Association,* . Retrieved from Bangkok:

Kampes, B. M. (2006). *Radar Interferometry - Persistent Scatterer Technique*: Dordrecht, Netherland: Springer.

Kulp, S. A., & Strauss, B. H. (2019). New elevation data triple estimates of global vulnerability to sea-level rise and coastal flooding. *Nature Communications, 10*(1). doi:10.1038/s41467-019-12808-z

Mohamadi, B., Balz, T., & Younes, A. (2019). A model for complex subsidence causality interpretation based on PS-InSAR cross-heading orbits analysis.

Remote Sensing, 11(17). doi:10.3390/rs11172014

Morley, C. K. (2015). Five anomalous structural aspects of rift basins in Thailand and their impact on petroleum systems. *Geological Society Special Publication, 421*(1), 143-168. doi:10.1144/SP421.2

Nutalaya, P., Chandra, S., & Balasubramaniam, A. (1984). Subsidence of Bangkok clay due to deep well pumping and its control through artificial recharge. *Land subsidence. Proc. 3rd symposium, Venice, 1984*, p727-744. doi:10.1016/0148-9062(88)92699-x

Pepe, A. (2007). *Advanced differential interferometric SAR techniques.* (Ph.D),

Pepe, A., & Calò, F. (2017). A review of interferometric synthetic aperture RADAR (InSAR) multi-track approaches for the retrieval of Earth's Surface displacements. *Applied Sciences (Switzerland), 7*(12). doi:10.3390/app7121264

Perissin, D. (2008). Validation of the submetric accuracy of vertical positioning of PSs in C-band. *IEEE Geoscience and Remote Sensing Letters, 5*(3), 502-506. doi:10.1109/LGRS.2008.921210

Perissin, D. (2016). *Interferometric SAR Multitemporal Proceeding: Techniques and Applications.* Paper presented at the Springer, Cham, Switzerland.

Perissin, D., Wang, T., Ferretti, A., Piantanida, R., Piccagli, D., Prati, C., . . . Zan, F. d. (2012). Repeat-pass SAR interferometry with partially coherent targets. *IEEE Transactions on Geoscience and Remote Sensing, 50*(1), 271-280. doi:10.1109/TGRS.2011.2160644

Perissin, D., Wang, Z., & Wang, T. (2011). The SARPROZ InSAR tool for urban subsidence/manmade structure stability monitoring in China. *34th International Symposium on Remote Sensing of Environment - The GEOSS Era: Towards Operational Environmental Monitoring*.

Phien-wej, N., Giao, P. H., & Nutalaya, P. (2006). Land subsidence in Bangkok, Thailand. *Engineering Geology, 82*(4), 187-201. doi:10.1016/j.enggeo.2005.10.004

Piromthong, P. (2015). *Detection of 1996-2000 rates and trend of land subsidence in Greater Bangkok by InSAR time-series analysis.* (Master's dissertation), Chulalongkorn University, Bangkok.

Samieie-Esfahany, S., Hanssen, R. F., Thienen-visser, K. V., Muntendam-bos, A., Samiei-Esfahany, S., Hanssen, R. F., . . . Muntendam-bos, A. (2010). On the effect of horizontal deformation on InSAR subsidence estimates. *Proceedings of Fringe 2009 Workshop, 2009*(March), 1-7.

Satirapod, C. (2020). *International Seminar: Bangkok The Underwater City "Countermeasures"; Sinking Bangkok: Engineering Viewpoint*. Retrieved from Bangkok, Thailand:

Schaufler, S., Bauer-Marschallinger, B., Hochstöger, S., & Wagner, W. (2018). Modelling and correcting azimuthal anisotropy in sentinel-1 backscatter data. *Remote Sensing Letters, 9*(8), 799-808. doi:10.1080/2150704X.2018.1480071

Searle, M. P., & Morley, C. K. (2019). Tectonic and thermal evolution of Thailand in the regional context of SE Asia. *The Geology of Thailand, 2019*(August), 539-571. doi:10.1144/goth.20

Simons, M., & Rosen, P. A. (2015). *Interferometric Synthetic Aperture Radar Geodesy* (Second Edition ed. Vol. 3). California Institute of Technology, Pasadena, CA, USA: Treatise on Geophysics.

Sinsakul, S. (2000). Late Quaternary geology of the Lower Central Plain, Thailand. *Journal of Asian Earth Sciences, 18*(4), 415-426. doi:10.1016/S1367-9120(99)00075-9

Snoeij, P., Attema, E., Davidson, M., Duesmann, B., Floury, N., Levrini, G., . . . Rosich, B. (2010). Sentinel-1 radar mission: Status and performance. *IEEE Aerospace and Electronic Systems Magazine, 25*(8), 32-39. doi:10.1109/MAES.2010.5552610

Spata, A., Guglielmino, F., Nunnari, G., & Puglisi, G. (2009). A new global approach to obtain three-dimensional displacement maps by integrating GPS and DInSAR data. *Proc. 'Fringe 2009 Workshop', 11*(2), 5890.

Torres, R., Snoeij, P., Geudtner, D., Bibby, D., Davidson, M., Attema, E., . . . Rostan, F. (2012). GMES Sentinel-1 mission. *Remote Sensing of Environment, 120*(The Sentinel Missions - New Opportunities for Science), 9-24. doi:10.1016/j.rse.2011.05.028

Trisirisatayawong, I., Naeije, M., Simons, W., & Fenoglio-Marc, L. (2011). Sea level change in the Gulf of Thailand from GPS-corrected tide gauge data and multi-satellite altimetry. *Global and Planetary Change, 76*(3-4), 137-151.

Werner, C., U. Wegmuller, T.Strozzi, A.Wiesmann. (2003). *Interferometric Point Target Analysis for Deformation Mapping.* Paper presented at the nterferometric Point Target Analysis for Deformation Mapping." In International Geoscience and Remote Sensing Symposium (IGARSS), Toulouse, France.

Wright, T. J., Parsons, B. E., & Lu, Z. (2004). Toward mapping surface deformation in three dimensions using InSAR. *Geophysical Research Letters, 31*(1), 1-5. doi:10.1029/2003GL018827